SKRIFTER NR. 186

Torgny Vinje and Øyvind Finnekåsa

The Ice Transport through the Fram Strait

ICEXAIR CAPSULE

NORSK POLARINSTITUTT
OSLO 1986

SKRIFTER NR. 186

Torgny Vinje and Øyvind Finnekåsa

The Ice Transport through the Fram Strait

ICEXAIR CAPSULE

NORSK POLARINSTITUTT
OSLO 1986

Contents

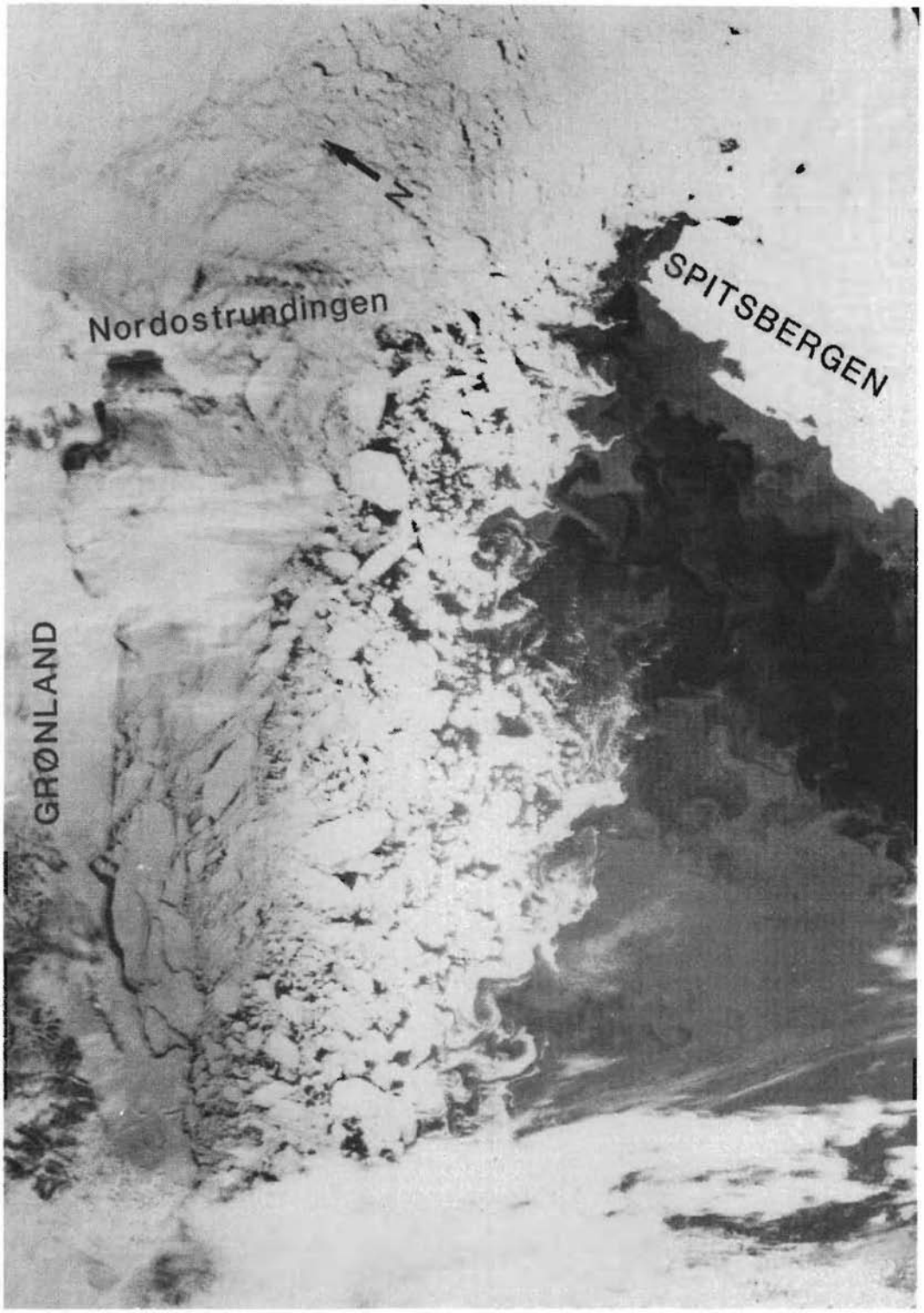

A composite visual and infra-red NOAA image displaying the ice drift stream in the Fram Strait on 14 May 1981, during conditions with a fairly northerly wind. The temperature difference between the warmer (dark) and the polar water is about 6° C.

Abstract

Based on surface observations, satellite information, and 52 ice drift tracks, the characteristic features of the ice transport through the Fram Strait are discussed. While the surface currents account for about 50% of the total ice drift in the central part of the Arctic Ocean (e.g. Thorndike & Colony 1982) it is found that this percentage increases towards 80 when the ice passes the Fram Strait. The cross-strait drift speed profile along 81° N shows a maximum between 5° and 10° W, i.e. along the shelf break off Greenland. In this area of maximum speed the ice velocity is fairly well correlated with intensity of the atmospheric circulation in the Norwegian-Greenland Sea.

The average seasonal ice export varies from a minimum in August of 0.09 mill. $m^3 s^{-1}$ to a maximum in January of 0.19 mill. $m^3 s^{-1}$ for the period considered (1976-1984). The mean annual export across 81° N is calculated at 0.159 mill. $m^3 s^{-1}$, or 5000 km^3 per year. This figure can be compared vith Koerner's (1973) estimate of 0.177 mill. $m^3 s^{-1}$, based on surface observations across the Arctic Ocean, with Østlund & Hut's (1984) calculations, 0.165 mill. $m^3 s^{-1}$, obtained from mass balance studies of isotope data, and finally with Ivanov's (1976) estimate of 0.134 mill. $m^3 s^{-1}$, of the net fresh water input to the Arctic Basin from runoff, precipitation, and evaporation. All figures are in ice equivalents.

1. Introduction

The major part of the ice that leaves the Arctic Ocean is conveyed with the Transpolar Ice Drift Stream which emerges through the Fram Strait. This ice stream, which continues further southward as the East Greenland Ice Drift Stream, is without comparison the largest and most concentrated meridional ice flow in the world. Its influence is to a varying degree felt both locally and regionally, and its magnitude is of such an order that its variation should also affect the global climate.

Satellite technology and improved logistic ability have radically improved the accessibility to the Fram Strait. New information as well as new types of data have been collected. This paper gives an outline of previous estimates, discusses various features of importance for the drift pattern, and recent observations and material used for the determination of the outflow of ice through this passage.

1.1. Previous estimates

Numerous estimates have been made of the ice transport through the Fram Strait, based on drift observations within the Arctic Ocean and assuming a certain deformation in the ice field when passing the Strait. Most of the estimates show values around 1 mill. km^2 year^{-1}. Gordienko & Karelin (1945), for instance, estimated an annual ice export of 1.036 mill. km^2 during the period 1933-1944 and Volkov & Gudkovic (1967) arrive at an ice export of 0.900 mill. km^2 year^{-1} from drift data obtained during the period 1954-1964.

Based on budget studies of the ice cover of the Arctic Ocean, Koerner (1973) estimated an annual outflow of 1.508 mill. km^2 with a mean ice thickness of 3.7 m, and the dynamic thermodynamic sea ice model of Hibler (1979) suggests an annual export of 1.211 mill. km^2 with a mean maximum ice thickness of 2.66 m.

Zacharov (1976) reports considerably lower values. He uses a constant speed for the ocean current (not given) and calculates the wind drift in the Fram Strait. He reports a seasonal variation with a maximum in the winter half-year and a minimum in the summer half-year with an average of 0.65 mill. km^2 per year.

Early observations of drift speeds in the Fram Strait itself were obtained during the North Pole I expedition in December 1937 (Papanin 1948?) and from the ice island ARLIS II in January 1965 (Ostenso & Pew 1968). From 1967 on it has been possible to determine the drift of ice floes from satellite imagery. Drift speeds over relatively short periods of 5—10 days were observed to vary considerably, both cross-stream and downstream, yielding extreme average export values of about 600 km^2 day^{-1} during the summer, and 6000 km^2 day^{-1} during the spring. Short timescale variations over a week, for instance, may range between 5800 and 2900 km^2 day^{-1}. Based on satellite observations of ice floe drifts and the width of the ice stream, Vinje (1982) suggests an annual mean export of 1.08 mill. km^{-2}, which is of the same order as most of the previous estimates based on drift observations in the Arctic Ocean.

The first estimate of volume transport based on measurements in the Fram Strait is given by Wadhams (1983). He combines the latest submarine ice thickness profile with an ice drift profile obtained from floe drifts by Vinje (1977). This drift profile which represents conditions with fairly strong northerly winds, yields accordingly the fairly high transport rate of 0.29 mill. m^3 s^{-1}. Wadhams gives an average ice thickness of 4.06 m and the corresponding ice area transported through the Strait thus becomes about 6200 km^2 day^{-1}, which is a slightly higher value than the maximum given above.

1.2. Special features

1.2.1. Fracture patterns. — Some characteristic features influence the ice transport through the Fram Strait. The most conspicuous one is the effect of the constriction on the drift pattern when the ice stream is accelerated by northerly winds (e.g. Shapiro & Burns 1975; Vinje 1977). This may best be visualized during the cold season when remote forces propagate more easily through the ice fields because of the better coupling between the individual floes at that time of the year (Fig. 1). Arching fractures are seen to run

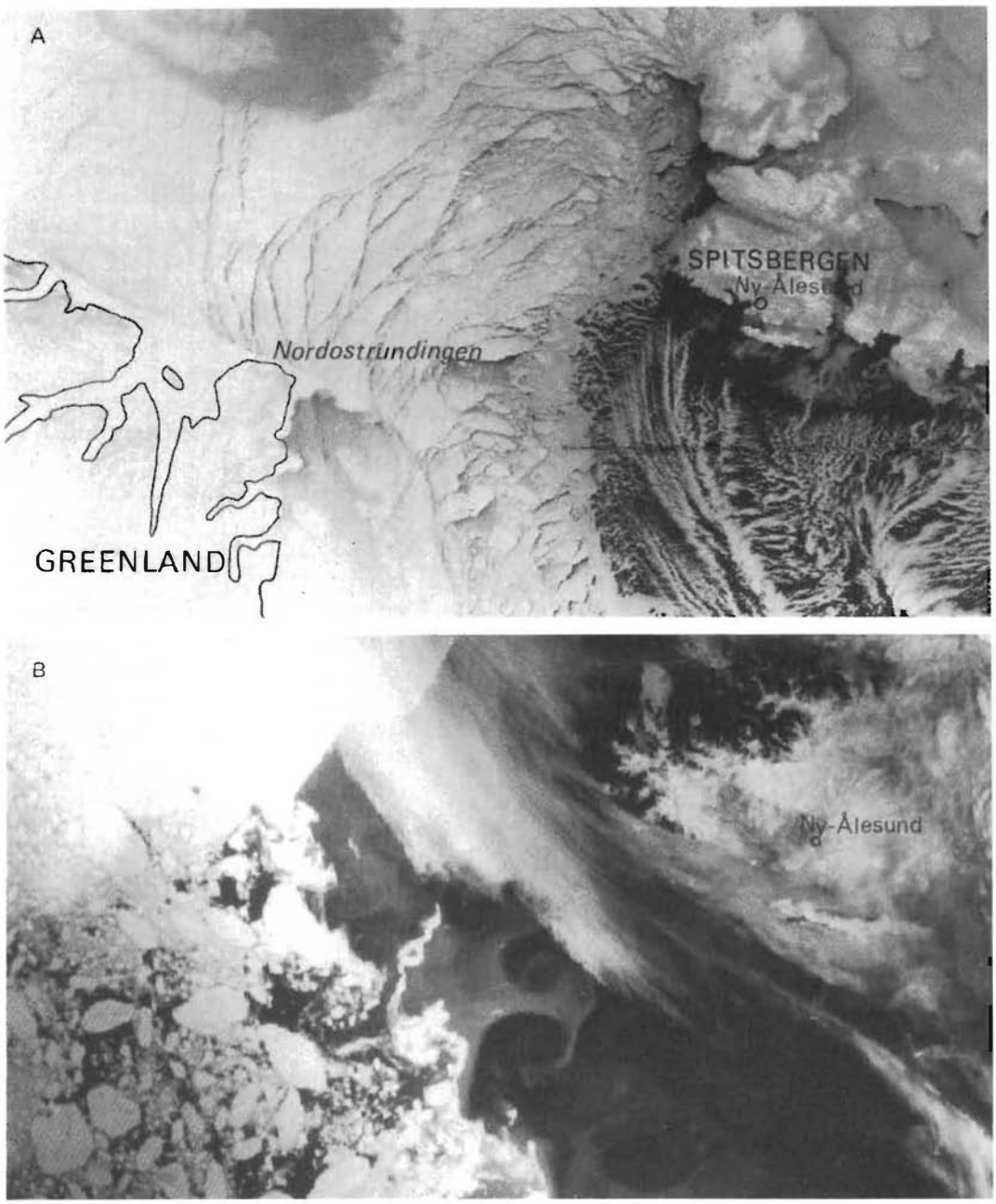

Fig. 1. A. Daylight NOAA-6 image obtained at Tromsø Satellite Telemetry Station on 2 March 1981 during an outbreak of polar air. We note the numerous parallelepiped-shaped ice floes in the north and the banding along the ice margins in the south of the Fram Strait. The characteristic fracture arching north of the passage seems to extend far into the Arctic Ocean. Note also the large areas of less disturbed ice along the Greenland coast. This undisturbed area seems to extend southwards from the grounded ice feature east of the Nordostrundingen polynya which at this time was covered with grey-white ice.

B. A NOAA-7 composite of daylight and infra-red images received in Tromsø on 27 June 1983. Note the eddy formations along the ice margins as well as along the oceanic Polar Front and, in particular, the well marked cyclonic and anticyclonic vorticity attached to the southeastward protruding branch of colder water above the Molloy Deep, west-northwest of Svalbard.

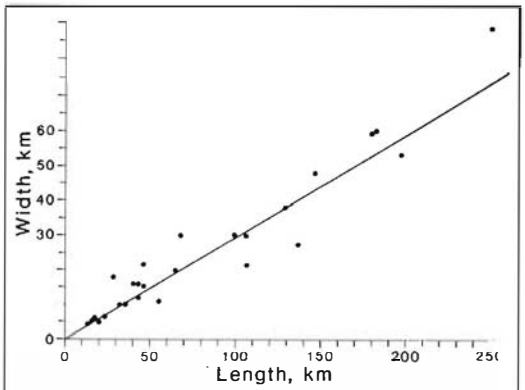

Passage	Ice floes Width /length	Width
Kvitøya–Nordaustlandet (Vinje 1977)	0.49	60 km
Fram Strait (see figure caption)	0.30	450 km

Fig. 2. Relation between breadth (B) and length (L) of the parallelepiped-shaped ice floes as observed north of the Fram Strait.

across the Strait from both sides, forming numerous parallelepiped-shaped floes. It is interesting to note that a similar slip line field is observed by Johnson & Kudo (1962) in a perfectly plastic material when extruded through a constrictive channel. Pritchard et al. (1979) have successfully used a plastic model to analyse the collapse of a sea ice arch in the Bering Strait.

There seems to be a fair correlation between the breadths (B) and the lengths (L) of the parallelepiped-shaped floes. A comparison with previous observations suggests a decrease in the quotient B/L with increasing width of the passage, from 0.49 for the 60 km wide passage between Nordaustlandet and Kvitøya (Vinje 1977) to 0.30 for the 450 km wide Fram Strait. The upper limit of L seems to be comparable with the half-width of the passage (Fig. 2).

The acute angle between the fractures and the friction borders can be estimated from simple kinematic reasoning given in textbooks. We choose the ordinate (y) along-stream and the abscissa (x) cross-stream. Assuming the drift speed (v) to increase linearly cross-stream we have

$$v = v_1 + mx$$

A point (x,y) will have moved after a time (t) to (x,y + vt), and a circle with a radius a, will be deformed to an ellipse. With a translation of $v_1 t$ and inferring for v, we get:

$$x^2 + (y + mtx)^2 = a^2$$

The angle θ between the x-axis and the short axis of the ellipse is given by $\operatorname{tg} 2\theta = 2/mt$. To begin with, at time $t = 0$, the angle becomes $\theta = 45°$. The ice is stretched along the long axis of the ellipse and fractures are formed perpendicularly, i.e. parallel to the short axis which at $t = 0$ forms an angel of 45° with the ice drift. This means that if the current increases linearly with the distance from the coast, the drag on the ice should cause an internal stress directed 45° to the left of the ice drift. This result is in good accordance with observations in newly broken ice near the friction borders along the Greenland coast (Figs. 1 and 3).

1.2.2. Local ice formation. — Because of the acceleration of the ice drift speed in the Fram Strait a persistent divergence in the ice field occurs during conditions with northerly winds. This should cause a persistent formation of new ice in this area in the cold seasons and markedly affect the composition of the ice fields in the Greenland Sea (e.g. Einarsson 1972). Divergences between 1 and 3×10^{-7} s^{-1}, calculated from satellite images obtained during the spring, correspond to a growth of new openings between 0.7% and 2% of a given area per day (Vinje 1970—1977). Assuming a residence time of about 20 days between 80° N and 78° N, the observed divergences suggest a possible new ice formation in 15—40% of the area in this period. The percentage distribution of the relative radiance on a LANDSAT scene on 25 March 1973 (Fig. 4), shows further that about 25% of the area considered is covered by newly formed ice, i.e.dark, grey or grey-white ice. All these observations indicate that a considerable ice production occurs in this region, which is important to keep in mind when determining the ice export from the Arctic Ocean. These observations also show that an increased expansion of the ice drift stream in this area does not necessarily indicate an increased efflux from the Arctic Ocean as suggested by Vowinckel (1964) and Strübing (1968).

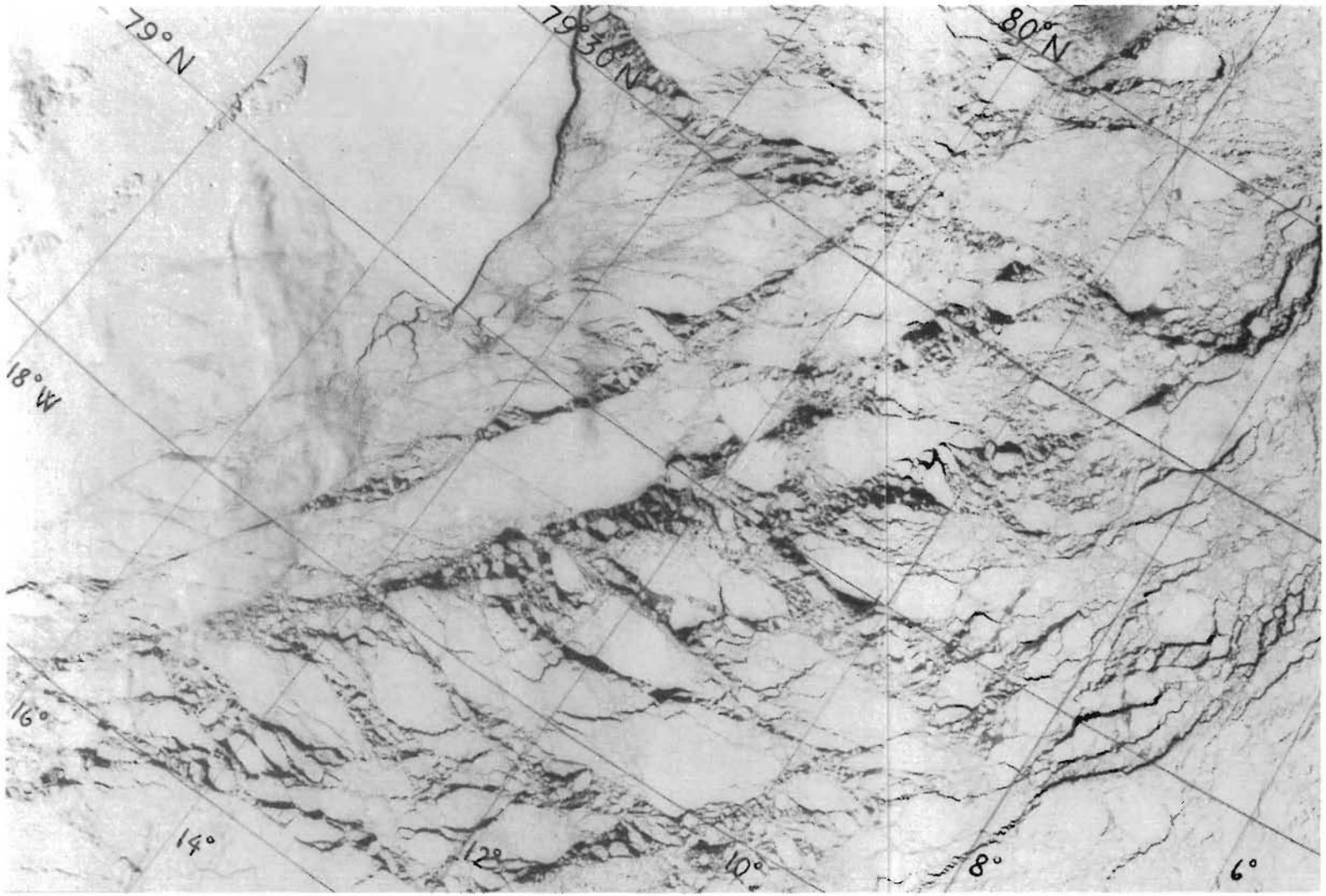

Fig. 3. Fracture patterns east of the coast of Greenland as observed by LANDSAT on 25 March 1976. The height of the picture is 185 km. Note the numerous 45° fracture angles relative to the slip lines.

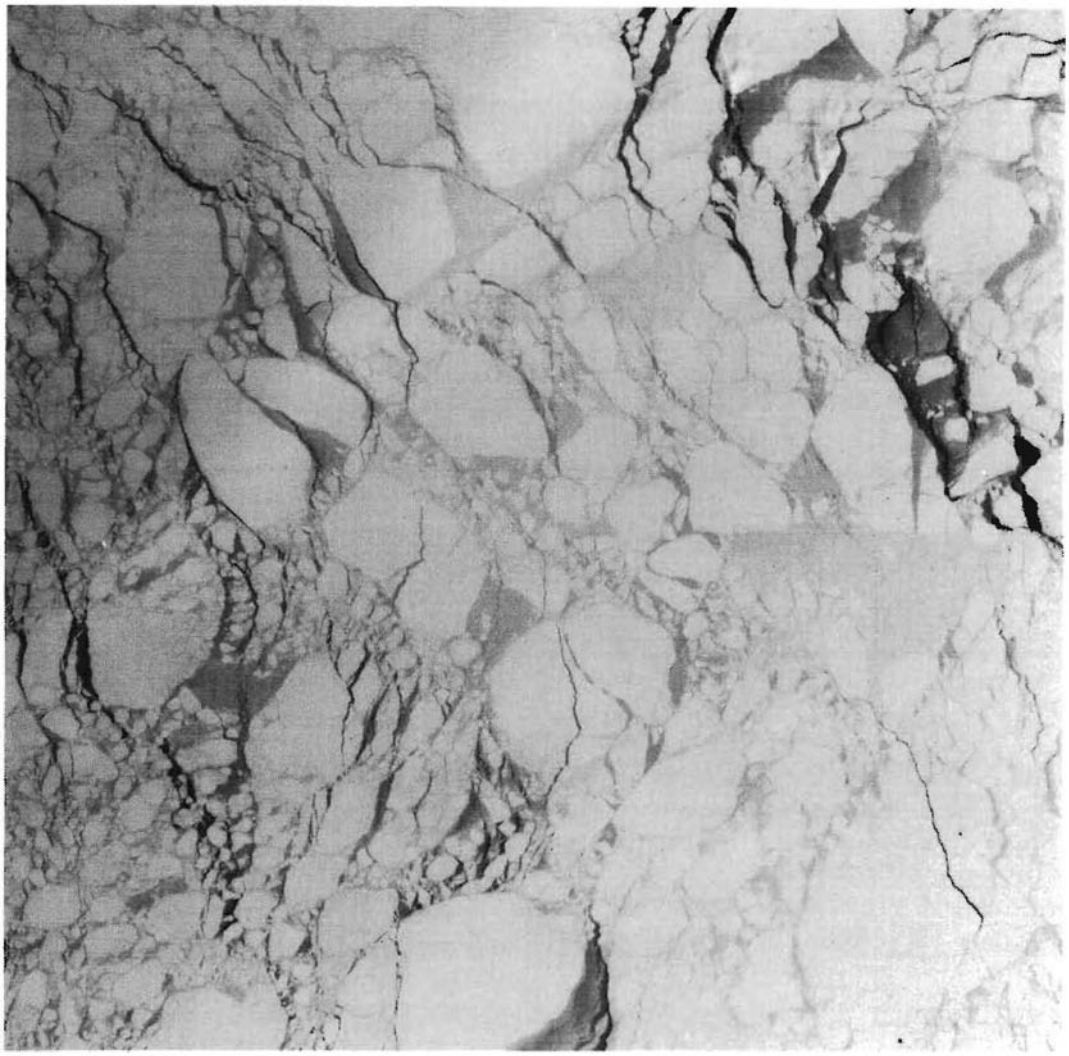

Fig. 4. The frequency distribution of the relative radiance as observed by LANDSAT 25 March 1973 in an area 185 km × 185 km centred at 78°35'N, 7°59'W in the East Greenland Ice Drift Stream. The amount of radiance coming from pixels with a relative radiance below 15 suggests that 25—30% of the area is covered with newly formed ice, i.e. dark, grey or grey-white ice.

1.2.3. Circulation over the Northeast Greenland Shelf. — The existence of an anticyclonic circulation over the Northeast Greenland Shelf as well as the coastal polynya south of Nordostrundingen has been known for some time (e.g. Riis-Carstensen 1938; Kiilerich 1945), and Laktionov & Yanes (1960) argue that this circulation is a semi-permanent feature. Additional hydrographic documentation of the anticyclonic circulation over the Northeast Greenland Shelf has been given by e.g. Palfrey (1967) and Newton (1983). This circulation is also clearly reflected in

the sea ice drift pattern observed in this area from satellite imagery (Fig. 5). Newton reports on relatively warm Intermediate Atlantic Water in the troughs north of the Belgica Bank. He suggests that a possible upward mixing would be responsible for the maintenance of the recurring polynya south of Nordostrundingen. Newton observed an anticyclonic circulation centered over Belgica Bank (78.5° N, 12° W), while our ice floe drifts from 1976 (Fig. 5) indicate a more northerly position of the centre that year. Palfrey's observations suggest a circulation with the centre in between.

Taking u and v as the horizontal velocity components, the vorticity (ζ) can be expressed by

$$\zeta = dv/dx - du/dy$$

Our ice drift observations (Fig. 5) thus give a vorticity around the center of the gyre of $-2.2 \times 10^{-6} s^{-1}$.

The polynya south of Nordostrundingen has been particularly frequent and well defined since October 1980. At that time an ice barrier was formed in an extension of Nordostrundingen. The length of this barrier was reduced considerably during a north-westerly gale around the beginning of August 1981. The remaining part was inspected in August 1984 and it turned out to consist of a mixture of tabular icebergs with heavily ridged sea ice in between (Vinje 1984; Fig. 6). Altogether 63 icebergs were observed of which three had capsized. Sixteen of the icebergs were measured and they showed lengths between 50 m and 400 m. The corresponding water depths and freeboards indicate iceberg thicknesses of between 60 m and 100 m. Assuming a partition of 1:8 between freeboard and thickness during free floating conditions, the excess freeboard of the icebergs indicates a forced vertical displacement in the order of 10 m. The length of this barrier, which may vary from year to year, has a clear influence on the ice drift pattern in the Fram Strait (Figs. 1 and 6). Satellite pictures indicate that the drift ice isthmus disappeared towards the end of September 1985.

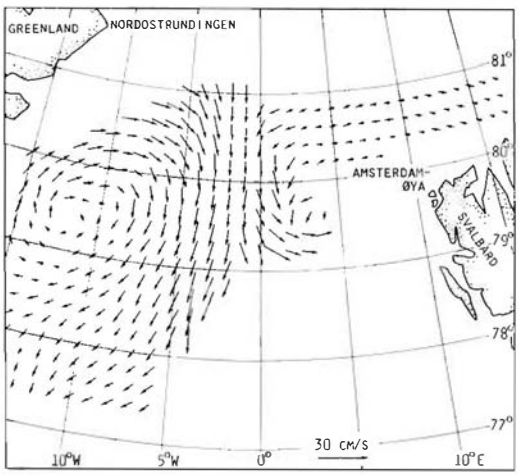

Fig. 5. Interpolated ice drift vectors based on daily observations of nearly 100 ice floes as traced on LANDSAT images during two periods with calm weather, 5—16 May 1—12 June 1976 (from Vinje 1977).

The origin of the icebergs is uncertain. However, provided the bottom topography allows it, the backwater circulation in the area suggests that icebergs might be transported to this area from glaciers located to the south. Massom (1984) has made a literature review of previous iceberg sightings in the area.

1.2.4. Ice edge eddies. — A frequent eddy formation takes place along the eastern border of the ice stream in the Fram Strait, particularly between 79° N and 80° N (e.g. Vinje 1982; Fig. 7). It is assumed that this phenomenon, which is frequently observed at the same geographical location, is caused by the particularly rough bottom topography in the area initiating disturbances on the polar front which, according to Griffiths & Linden (1982), is unstable along its whole length in the Greenland Sea. Well defined cyclonic eddies were reflected in the sea ice distribution observed in this area on LANDSAT images in May 1976 (Fig. 7). Later that summer, one of our ice drift buoys circulated in the area from 20 June to 30 July, observing a thermal structure in the surface layer similar to that of a cyclonic vortex (Vinje 1982). Also, in October of that year, sound velocity profiles obtained from a submarine indicated warmer water within the zone of Polar Water, suggesting the presence of an eddy (Wadhams et al. 1979). Later on, eddy formations in this area, near or over the Molloy Deep, have been observed rather frequently, also on weather satellite images (cf. Fig. 1). Profiles of temperature and salinity observed in 1980 in

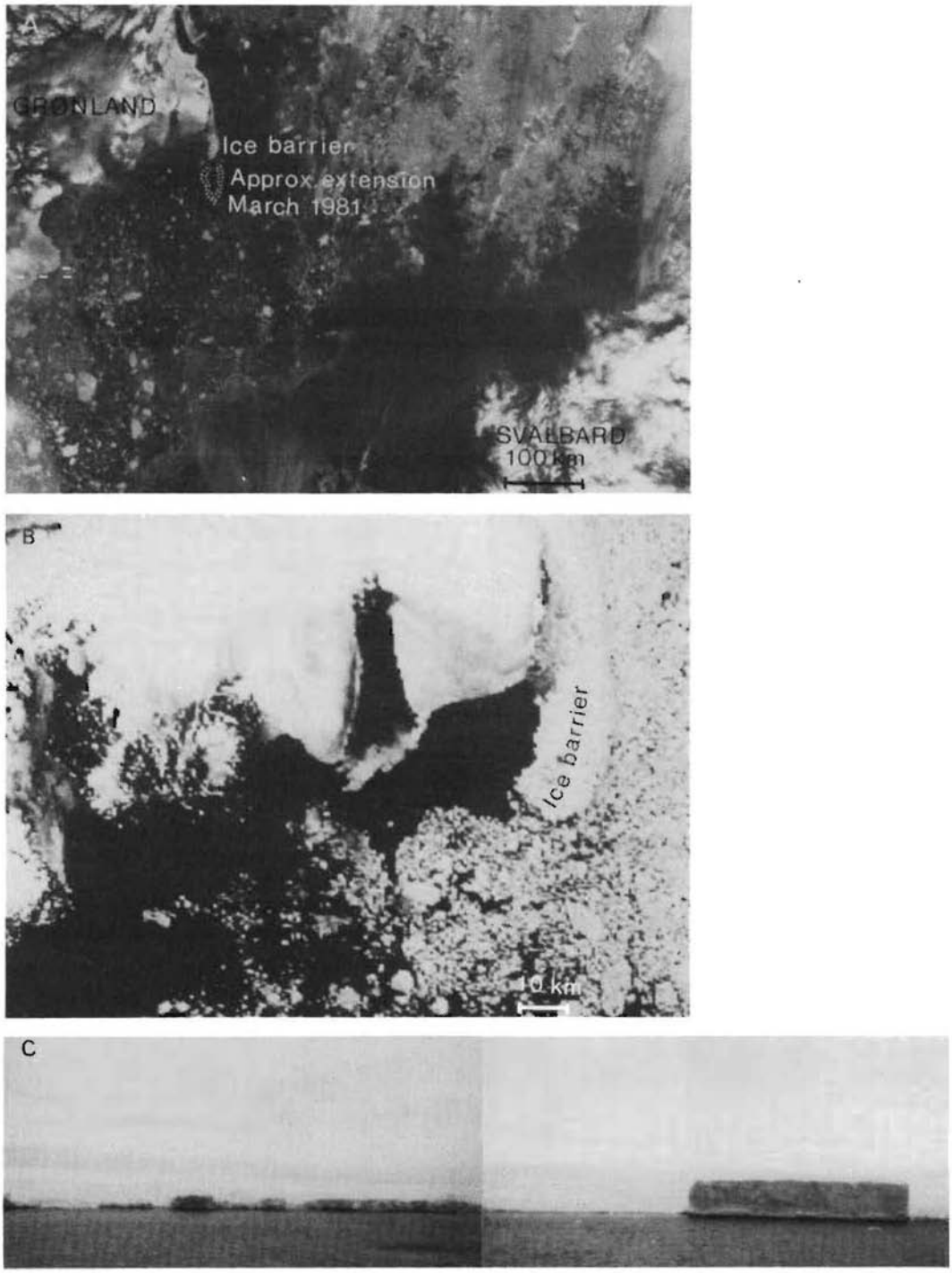

Fig. 6. The ice barrier extending from Nordostrundingen. *A.* A NOAA-7 satellite image received in Tromsø on 24 August 1984. Note the approximate extension of this feature as observed in March 1981. *B.* A LANDSAT image received at Kiruna on 20 July 1983 showing the ice barrier as well as the sheltered, ice free area to the south of it. *C.* The ice barrier seen towards the north at 81° 13'N, 10°04'W on 25 August 1984 from LANCE. The height of the grounded tabular iceberg above the sea surface is 18 m. The water depth is 73 metres suggesting a total thickness of 90 m.

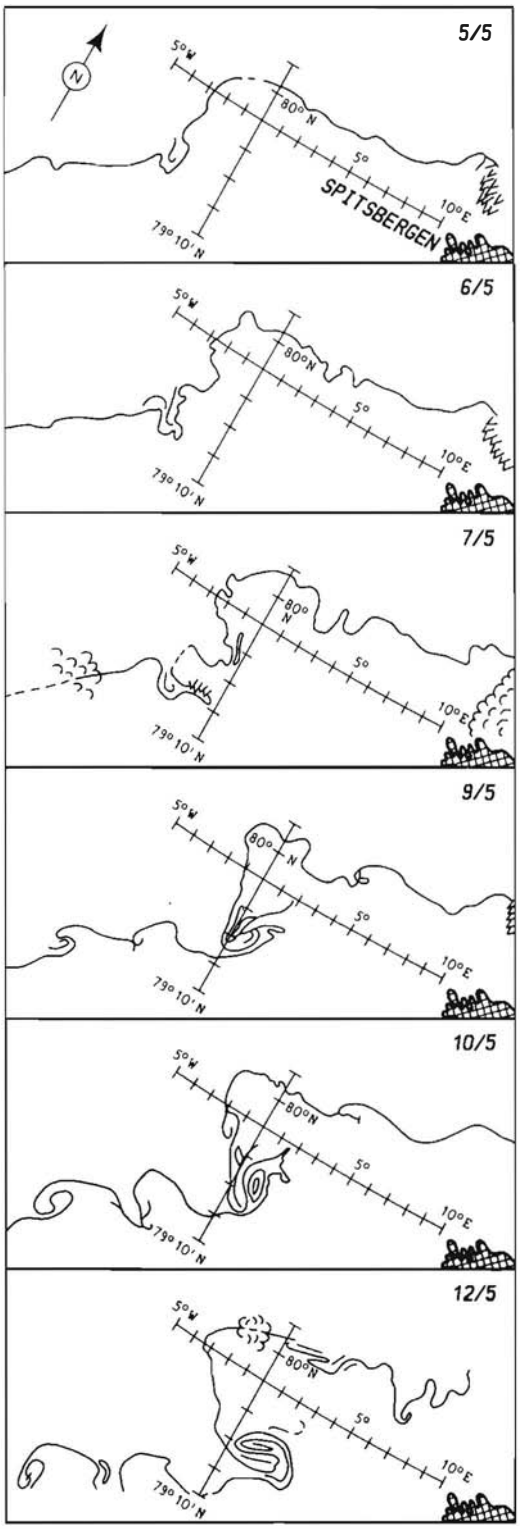

an ice vortex feature just west-northwest of this location would suggest an eddy produced by a baroclinic instability in the polar front (Wadhams & Squire 1983). Applying the concept of conservation of potential vorticity and assuming some simplifications on the bottom topography constraints, Smith et al. (1984) calculate the effect of a bottom depression on the surface circulation. Their two-layer model suggests a development of a cyclonic circulation. While the flow is initially barotropic, a baroclinic component does develop. The estimated surface vorticity, as calculated from this model of 5.8×10^{-5} s^{-1}, is in accordance with the visual observations of eddy developments in this area described below.

The well-defined vortex observed on 9 May 1976 (Fig. 7) revolved about 130° anticlockwise and performed an eastward translation of 10 km per day, between 9 and 12 May. The long and the short axis of the eddy are about 30 and 15 kilometres, respectively. The corresponding vorticity, is thus 2×10^{-5} s^{-1}. The new-formed eddy to the south of the largest one indicates a velocity perpendicular to the main ice edge of 0.30 m s^{-1} as an average over a period of 24 h. Assuming that this speed is reduced to zero over the half-width of the protruding tongue, we get a positive/negative vorticity in the order of 5.8×10^{-5} s^{-1} to the north/south of the central core of this tongue. The shape of the newly formed eddy shows most markedly a cyclonic circulation on the northern side of the tongue. However, an anticyclonic circulation is also indicated on its southern side. According to the principle of the conservation of potential vorticity the latter circulation should be expected to develop when the currents are moving away from the Molloy Deep. Protruding tongues of ice or colder water with opposite circulations on the two sides may be very well developed on some occasions (Figs. 7 and 1).

The eddies formed along the ice edge will cause a lateral leakage of ice from the East Greenland Ice Drift Stream. The cross-edge transport by the eddy to the south of the main one, during the primary stage of its development,

Fig. 7. A sequence of LANDSAT images showing the evolution of ice edge eddies over or near the Molloy Deep in the Fram Strait, 5—12 May 1976. See text for explanation.

is calculated to be about 350 km² per day (Fig. 7). Similar areas of detached ice are seen to be contained also in the eddies further to the south, while a somewhat greater cross-edge transport is indicated by the main eddy. The main eddy seems to affect the sea ice distribution, initially on 5 May. By 12 May the detached ice field is registered only faintly on the LANDSAT image. This would suggest that most of the ice in this eddy has melted over a period of seven days under the forced contact with warmer water. Assuming a detachment of 350 km² per eddy, and a lifetime of about ten days before the ice melts, we arrive at a lateral transport, caused by the four eddies, of about 50 km² per day per 100 km ice edge. An increased leakage is caused by the wave effects and by the disintegration of ice bands which are formed during conditions with off-ice winds (Wadhams 1981 b; cf. also Fig. 1).

1.3. Momentum balance

The most commonly used relationship for determination of the wind and current effects on the total ice drift is

$$\mathbf{U} = A\mathbf{G} + \mathbf{c} \tag{1}$$

where **U** and **G** are the vectors of ice drift and the geostrophic wind, respectively, **c** is the non-wind effects, here referred to as the average surface current, and A is the geostrophic wind factor. This relationship, which according to Thorndike & Colony (1982) fits the observations just as well as the more solidly founded momentum balance equation, will also be used in the present context. Because the current conditions are so special in the Fram Strait, we will, however, first consider the order of magnitude of the various terms with reference to the momentum balance equation:

$$\boldsymbol{\tau}_a + \boldsymbol{\tau}_w + \mathbf{C} + \mathbf{T} + \mathbf{F} = m\,D\mathbf{U}/Dt \tag{2}$$

Here $\boldsymbol{\tau}_a$ and $\boldsymbol{\tau}_w$ are the wind — and water stresses, respectively, **C** the Coriolis force, **T** the pressure gradient force due to the tilting of the surface. **F** the force due to the internal stress gradient, m the ice mass per unit area, and D**U**/Dt the substantial derivative.

The momentum balance equation is generally considered for stationary conditions when no acceleration occurs, i.e. the time derivatives are zero. Equation (2) has under this assumption been solved with appropriate simplifications by several investigators (e.g. Nansen 1902; Shuleikin 1938; Reed & Campbell 1962; McPhee 1980).

Direct observations as well as calculations show that relatively high accelerations take place in the Fram Strait (Papanin 1948; Ostenso & Pew 1968; Vinje 1977; Hibler 1979). A typical acceleration rate is 0.5×10^{-7} m s^{-2} (cf. p.17). With an ice density of 900 kg m^3 and an ice thickness of 4 m, the acceleration term in Equation (2) thus becomes in the order 10^{-4} kg m^{-1} s^{-2}. When considering shorter time spans, for instance in connection with eddy formation along the ice edge, the acceleration term may assume values which are at least a hundred times higher. This was, for example, the case during the eddy evolutions which took place between 9 and 12 May 1976 (Fig. 7).

The wind stress and water stress terms can be represented by the quadratic laws

$$\boldsymbol{\tau}_a = \varrho_a D_{10} (\mathbf{G}-\mathbf{U})^2$$
$$\boldsymbol{\tau}_w = \varrho_w D_w (\mathbf{c}-\mathbf{U})^2 \tag{3}$$

where we have neglected the air and water turning angles in connection with the determination of order of magnitude. With $\varrho_a = 1.3$ kg m^{-3}, $D_{10} = 0.009$ (McPhee 1980) and observed average differences between **G** and **U** (Table 3), the wind stress assumes values between 10^{-1} and 10^{-2} kg m^{-1} s^{-2}. Applying a drag coefficient for the ice-water interface of $D_W = 0.0055$ (McPhee 1980), the water stress assumes values in the order of 10^{-2} kg m^{-1} s^{-2} Assuming geostrophic balance, the Coriolis and the surface tilt terms will combine in the form (e.g. Neralla et al. 1980).

$$\mathbf{C} + \mathbf{T} = \varrho_i h_i f (\mathbf{k} \times (\mathbf{U}-\mathbf{c})) \tag{4}$$

where ϱ_i and h_i are the density and thickness of the ice, respectively, f the Coriolis parameter, and **k** the vertical unit vector. With the Coriolis parameter of 1.4×10^{-4} s^{-1} and ϱ_i and h_i as above, the order of magnitude of this combined term is also 10^{-2} kg m^{-1} s^{-2}.

The calculations made by Hibler & Bryan (1984) show an internal ice stress which is of the

same order as the current and wind stresses. The acceleration term, accordingly, becomes two orders of magnitude less than all the other terms in Equation (2). Hence, considering longer periods in confined areas, we can assume that stationary conditions are well approximated in the Fram Strait.

We shall below use the observations of **U** and **G** to estimate the wind factor A, the turning angle α, the mean surface current **c**, and the variance from the linear relationship (1). The variance will give information about the fluctuating effects of the internal stress gradients, ocean currents, and accelerations. As these fluctuating effects are assumed to be greater in the Fram Strait than in the Arctic Ocean, we should a priori expect to find a relatively lower correlation between **U** and **G** in the marginal areas as compared with the interior.

2. Observations

A Norwegian «Ice Drift Experiment» (ICEX) started in 1976 as part of a national contribution to the GARP polar programmes. The main aim of the experiment is to obtain information on an important climatic parameter: the export of ice from the Arctic Ocean through the Fram Strait. The project was reorganized in 1981, and became a joint programme between the Norwegian Polar Research Institute and the Norwegian Meteorological Institute, also involving cooperation with the University of Washington's «Arctic Ocean Buoy Program», which started in 1979.

The data base for the present investigation includes ICEX drift results as well as all other available information from recent and previous long-term drifts in the Fram Strait area. Altogether 52 ice drift tracks have been investigated of which 50 have been obtained from buoys and two from the manned stations North Pole I and ARLIS II.

An ICEX measuring capsule has been developed in co-operation with the Chr. Michelsens Institutt, Bergen (Vinje & Steinbakke 1976; Nergaard et al. 1985). The capsule operates effectively in the marginal sea ice areas where it may be subject to frequent ridging and sporadic drift in water. The buoys were deployed from a boat during a pilot project in 1975, from a Cessna 185 aircraft landing on the ice in 1976 and 1977, and from 1978 onwards they have been air-dropped by the Norwegian Air Force. To obtain information on the cross-strait ice thickness distribution, an ice observing programme has been carried out in the Fram Strait during the last four summers.

The ice drift data used in the present investigations are collected from various sources listed in Table 1.

Table 1. — Data sets used in the present investigation.

Year	No. of platforms	System	Platform or experiment	Reference
1937	1	Manned	North Pole I	Papanin (1948?)
1965	1	Manned	Arlis II	Ostenso & Pew (1968)
1976	4	RAMS	ICEX	Vinje & Finnekåsa (1986)
1977	2	RAMS	ICEX	Vinje & Finnekåsa (1986)
1978	3	RAMS	ICEX	Vinje & Finnekåsa (1986)
1979	1	RAMS	ICEX	Vinje & Finnekåsa (1986)
	3	ARGOS	ICEX	Vinje & Finnekåsa (1986)
	6	ARGOS	ICEX	Kloster & Rafto (1980)
	2	ARGOS	AOBP	Thorndike & Colony (1980)
1980	2	ARGOS	AOBP	Thorndike & Colony (1981)
1981	4	ARGOS	ICEX/AOBP	Thorndike et al. (1982)
1982	3	ARGOS	ICEX/AOBP	Thorndike et al. (1983)
1983	3	ARGOS	ICEX/AOBP	Colony & Munoz (1985)
	7	ARGOS	MIZEX	Symonds & Peterson (1985)
1984	10	ARGOS	MIZEX	Symonds & Peterson (1985)

ICEX: Norwegian Ice Drift Experiment
AOBP: Arctic Ocean Buoy Program
MIZEX: Marginal Ice Zone Experiment.

The first satellite tracked ICEX buoys were deployed in the Fram Strait in May 1976. The Random Access Measurement System (RAMS) on board NIMBUS-6 were used and the location was reported about ten times a day. According to a test made at Spitsbergen, about 90% of the positions were located within a distance of one kilometre from the average position (Vinje & Steinbakke 1976). However, some of the localizations were far outside this limit, and these observations were removed from the data set by a simple filtering procedure. The daily ice drift was determined from the difference in the daily mean positions.

When the ARGOS system came into use in 1979, the accuracy of the positioning had improved by about one order of magnitude, and filtering of the data was no longer necessary. The daily average ice drift is determined from the positions observed at 24 h intervals. An accuracy of about 200 m in each position and an average standard deviation of $U = 0.08$ m s^{-1} (Table 3) implies typical errors of about 0.005 m s^{-1} in the ice drift speed due to positioning errors.

2.1. Ice drift pattern

The annual average ice drift pattern represented in Fig. 8 is based on all the 52 drift tracks. Fig. 9 shows the average drift pattern for the months May—August.

A considerable increase of the ice velocity occurs in the Fram Strait. The acceleration in the central area, for example, between one and four degrees west, is 0.5×10^{-7} m s^{-2}. This figure is unexpectedly constant over the very long distance from 83° N to 78° N, and reveals an average drift speed increase of as much as one order of magnitude over the mentioned distance. We observe also, as should be expected, that the zone of maximum speed coincides with the maximum surface currents (Kiilerich 1945) located over the continental shelf break. This is also in accordance with the numerous ice floe drifts obtained from satellite pictures (e.g. Vinje 1970, 1977). The ice drift speeds are, however, in general, markedly less than Kiilerich's calculated current speeds.

The backwater circulation over the northeastern continental shelves of Greenland is reflected by the anticyclonic circulation at about 79.5° N, 12° W. Further north in this shelf area the ice drift seems to be less orderly with the occasional influx from the Arctic Ocean.

We note the relatively small average drift speed around 80° N and 2—5° E. This probably reflects the resultant effects of the southward moving Transpolar Current and the northward-moving West Spitsbergen Current, which submerge beneath the former in this area. (The higher speeds observed further east at this latitude are less representative in this connection due to the far fewer days included.)

The drift speed distribution along 79° N shows a maximum zone over the shelf break which is located at some distance inward from the outer ice margin. The drift speeds in the ice margin itself, which generally passes over the Molloy Deep at this latitude, seem to be somewhat reduced compared with the drift speed further to the west. Because of the increased wind effect on the more open ice cover in the margins, we should have expected the highest drift speeds here. The observed reduction for average conditions may, therefore, reflect a more or less persistent transfer of momentum from the main stream to the local eddying.

An area with a cyclonic turn in the average ice drift is located in the Greenland Sea near 75° N and 10° W. The ice motion is also here in accordance with the pattern of the surface currents as given by Kiilerich (1945). This ice drift feature is persistently reflected in the frequency distribution of sea ice in the area, particularly during the expansion period December-May (e.g. Vinje 1976, 1985), and it is therefore probably of a semi-permanent nature. It is located in the ice-free bight called Nordbukta, which in some years is extremely well developed, contemporary with the more southerly ice promotory called Odden (Vinje 1980; cf Fig. 17).

The average cross-strait drift speed profile is given in Table 2 for two different periods, May—August and September—April. The two periods show marked differences in the intensity of the atmospheric circulation, which is illustrated by the corresponding monthly average difference in air pressure between the Fram Strait (80° N, 15° W) and the central part of the Norwegian-Greenland Sea (73° N, 5° E). The daily average drift speeds within 0.5° north and south of the 81st parallel have been considered.

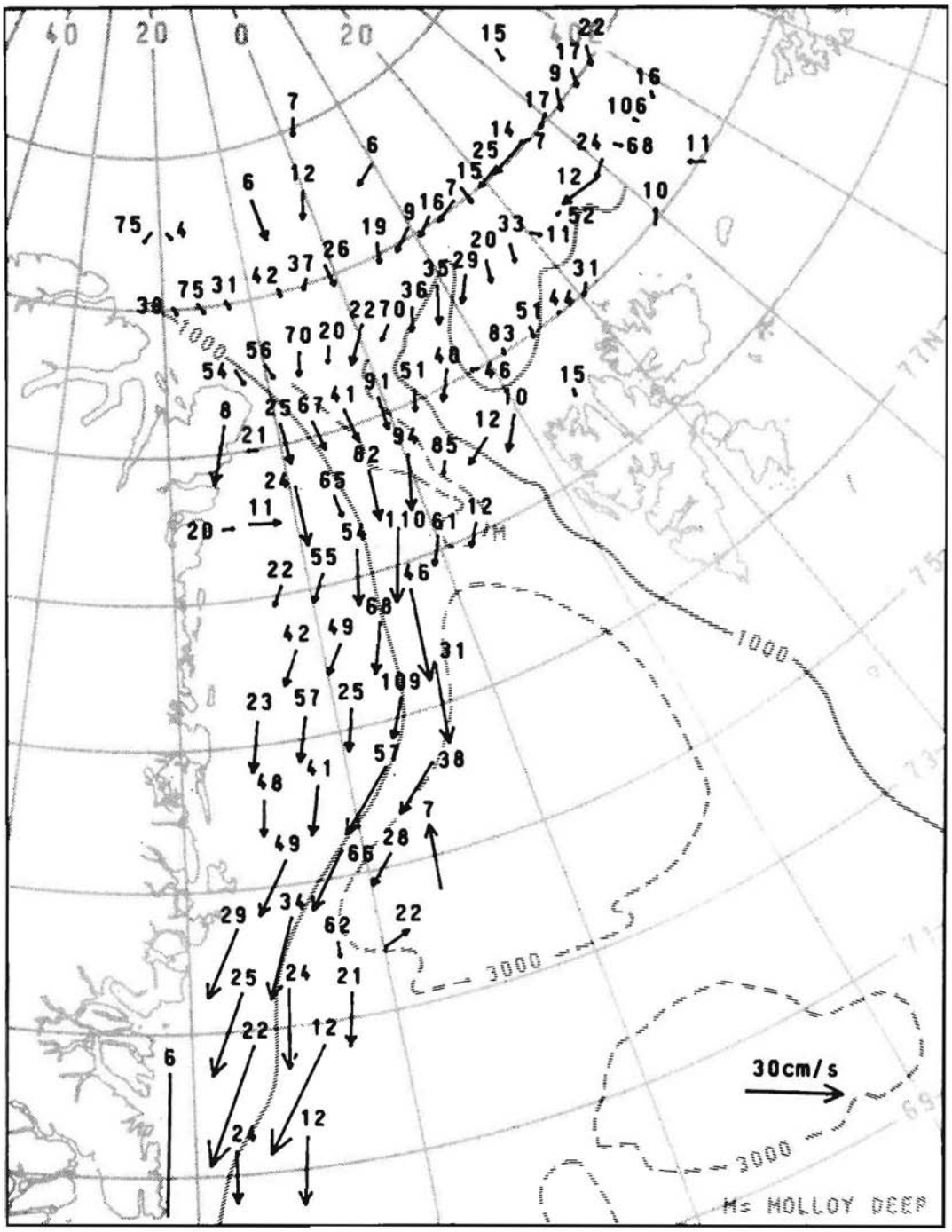

Fig. 8. The spatial distribution of ice drift vectors. The numbers give the daily average drifts used for the computation. The grid square is 3° longitude × 1° latitude.

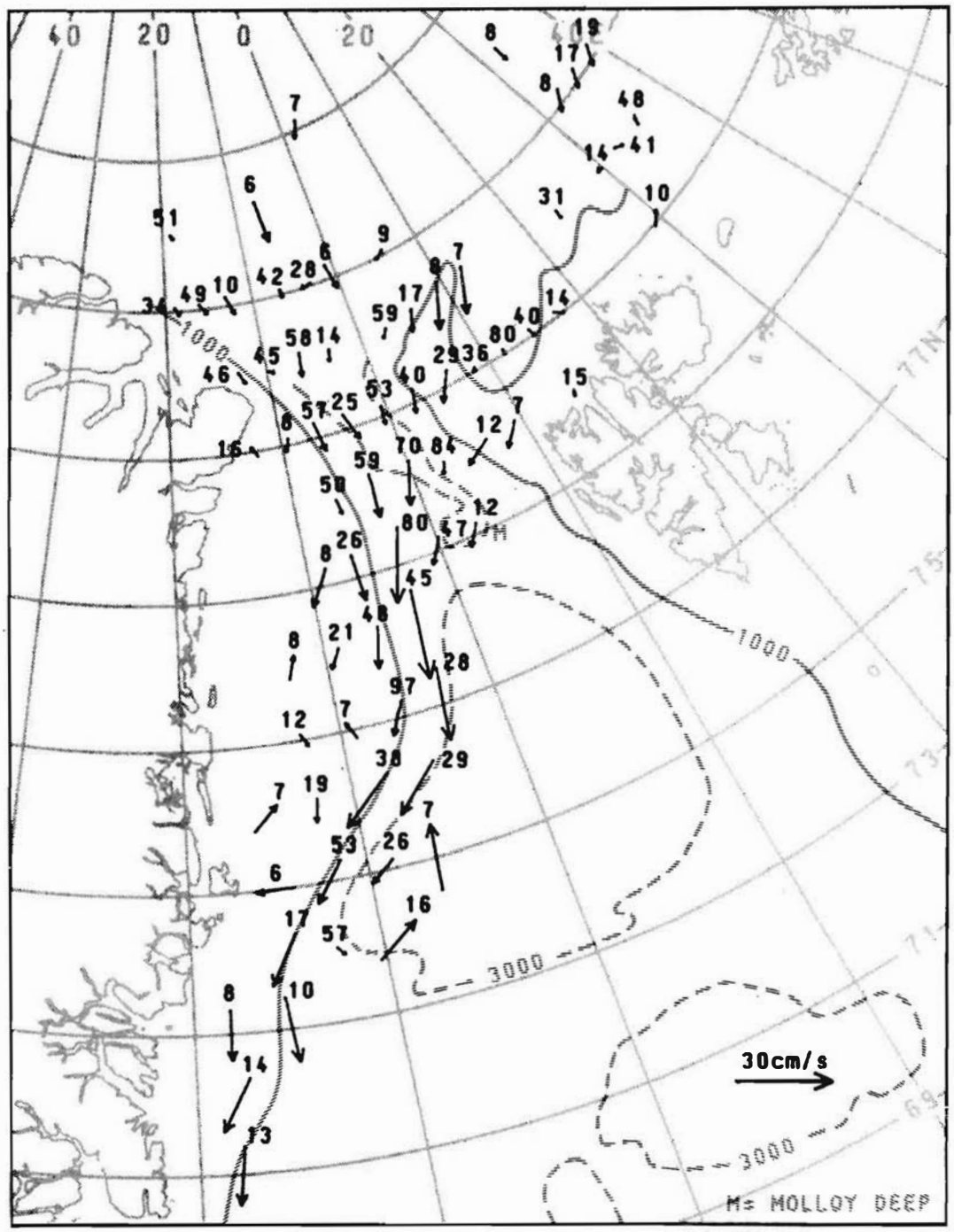

Fig. 9. The mean ice drift pattern based on daily averages obtained in the months May-August.

Table 2. — The cross-strait variation of the mean meridional component of the ice drift speed, Uy m s^{-1}, the standard deviation σUy, and the number of buoy-days, N, observed from the drifts of 43 buoys and two manned ice islands across the 81st parallel. The corresponding air pressure difference between the Fram Strait (81° N, 15° W) and the central part of the Norwegian-Greenland Sea (73° N, 5° E) is given by ΔP (mb).

	West		East				Number of drift tracks	ΔP
	10—5	5—0	0—5	5—10	10—15	15—21		
May—August								
Uy	0.081	0.066	0.065	0.054	0.020	0.018	24	0.7
σUy	0.090	0.082	0.073	0.091	0.058	0.081		
N	66	63	75	51	113	30		
September — April								
Uy	0.160	0.127	0.149	0.069	0.098	0.036	21	8.2
σUy	0.089	0.098	0.125	0.069	0.058	0.067		
N	30	37	35	13	16	49		

The average ice drift speed during the winter is nearly twice as high as the summer drift speed. The order of magnitude of the standard deviation seems to be independent of both longitude and season. This will be discussed further in the next section.

The average drift speed profile (Fig. 10) can be considered as a weighting function. This weighting function will be used later for calculation of the volume transport through the Strait.

2.1.1. Wind drift. —Nansen (1902) found from observations during the FRAM drift that the ice is moving at a velocity of about 2% of the surface wind speed and deflected from the wind direction 25—30° to the right. Because of the turning to the right of the wind with height and the deflection of the ice drift to the right of the surface wind, there occurs a merging in the directions of the ice drift and the wind above the surface friction layer. Zubov & Somov (1940) used this observation as the basis for a linear relationship between the ice drift and the air pressure gradient, yielding a wind drift equal to 0.9% of the geostrophic wind speed.

The wind drag on a surface is to a large extent determined by the roughness of the surface. According to measurements obtained with the aid of theodolites at Cap Smit over a period of

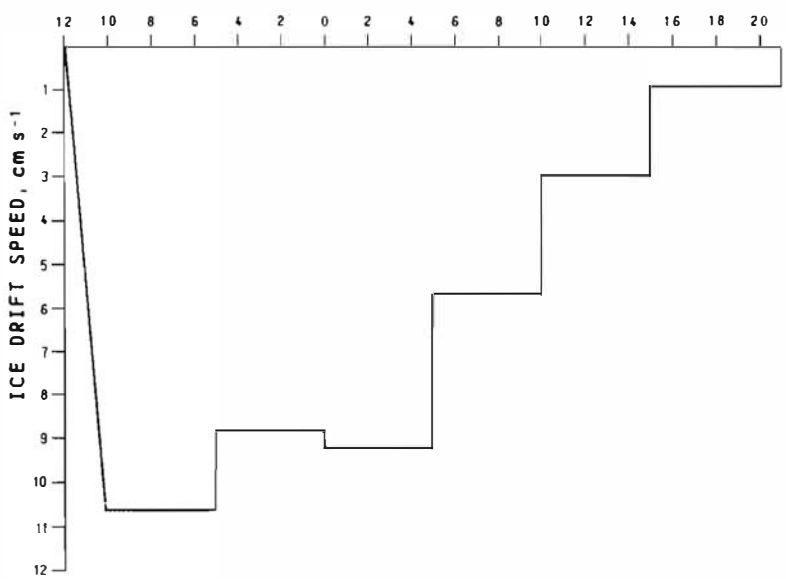

Fig. 10. The mean drift speed profile at 81° N in the Fram Strait based on the passage of 43 buoys and two manned stations. The number of drift days contained in the various longitudinal intervals are given in Fig. 8.

two years (Zubov 1943), the surface wind factor was found to increase by one order of magnitude as the ridging extent increased from 1/10 to 9/10 of the total area. The wind factor is less sensitive to ice concentration and decreases about threefold when the ice cover increases from 1/10 to 9/10. As the roughness may vary considerably from floe to floe in an ice field, we should expect the ice floes to perform more or less individual movements as long as they are not frozen or packed together. This may explain why certain ice floes move with a deviating angle and with a considerably higher speed than other floes during uniform wind conditions. Excess speeds of about 40%, together with a marked deviation in drift direction from the neighbouring floes of about 30°, have thus been observed in the marginal ice zone in the Fram Strait (Vinje 1977). A possible individual ice floe movement should be kept in mind as pertains to discussions on the representativeness or interpretation of ice drift measurements in relation to wind effects.

The geostrophic wind speed corresponding to the daily average ice drift has been extracted from the European Meteorological Bulletin (Deutscher Wetterdienst) for 1976, 1977, 1978, 1982, and 1983, and from Thorndike & Colony's data sets for 1979, 1980, and 1981. The MIZEX drift tracks as well as those from the two manned stations have not been included in this study. This investigation is also restricted to the drifts between 85° N and 75° N. All readings were given an index of reliability and only those with the highest score have been used for the determination of the geostrophic wind factor. Typical errors in the geostrophic wind speed estimates are 3 m s^{-1}.

It soon became evident that there is a considerable variation in the ice drift pattern from place to place, and that some special features are characteristic of confined areas. Because of this, we have considered the **U-G** relationships (Equation (1)) in five different domains of the experimental area (Fig. 11). This achieves a considerably lower value of the standard error of estimate.

The squared correlation coefficient expresses the percentage of the total variance which can be explained by changes in the geostrophic wind stress. There is a considerable variation in this figure from place to place and we note that the higher values, above 70%, are observed at distances more than 200 km from land (Fig. 11). The observations of Thorndike & Colony (1982) in the Arctic Ocean indicate a similar high value of the squared correlation at about twice this distance from the land margins. This difference, if real, might indicate an effect in the Fram Strait of the accelerating ocean currents and the corresponding reduced effect on the meridional component of the internal stress gradient in the diverging ice field. This view is supported by the fact that Hibler & Bryan (1984) calculated an internal stress gradient with little or no component along-stream in the central part of the East Greenland Ice Drift Stream.

The marked cross-stream variation of the explained variance in the strait (Fig. 11) suggests an increased influence of non-wind effects when approaching the coast on either side of the strait. The cross-stream variation further south suggests that the effects on the ice drift of variable currents or eddies are most clearly felt in the marginal sea ice zone, as should be expected. A very low percentage of the explained variance, about 16%, was, for example, observed for the buoy (ID 6236) which was trapped in the eddying area over the Molloy Deep in 1976, and also for the buoys with IDs 6072 and 1593 which drifted in the anticyclonic eddy over the Northeast Greenland continental shelf in 1976 and 1979, respectively (See Table 3). Short time accelerations of a considerable magnitude may also, as we have seen, take place in this area in connection with eddy formations and add substantially to the violation of an approximate linear relationship between ice drift and geostrophic wind for higher wind speeds.

Fig. 12 shows two examples of the relationship between the decomposed geostrophic wind and the ice drift components in the area north of the Barents Sea (Area A). The upper part of this figure shows the data sets which give some of the highest correlations observed in this investigation. During most of the period, March—October 1981, the buoy drifted in an area with a 9/10 ice cover. It is noted that the meridional movement of the ice does not seem to be hindered to a discernible extent by the row of islands to the south of Area A. As illustrated by the lower part of Fig. 12 the same observation is also made in

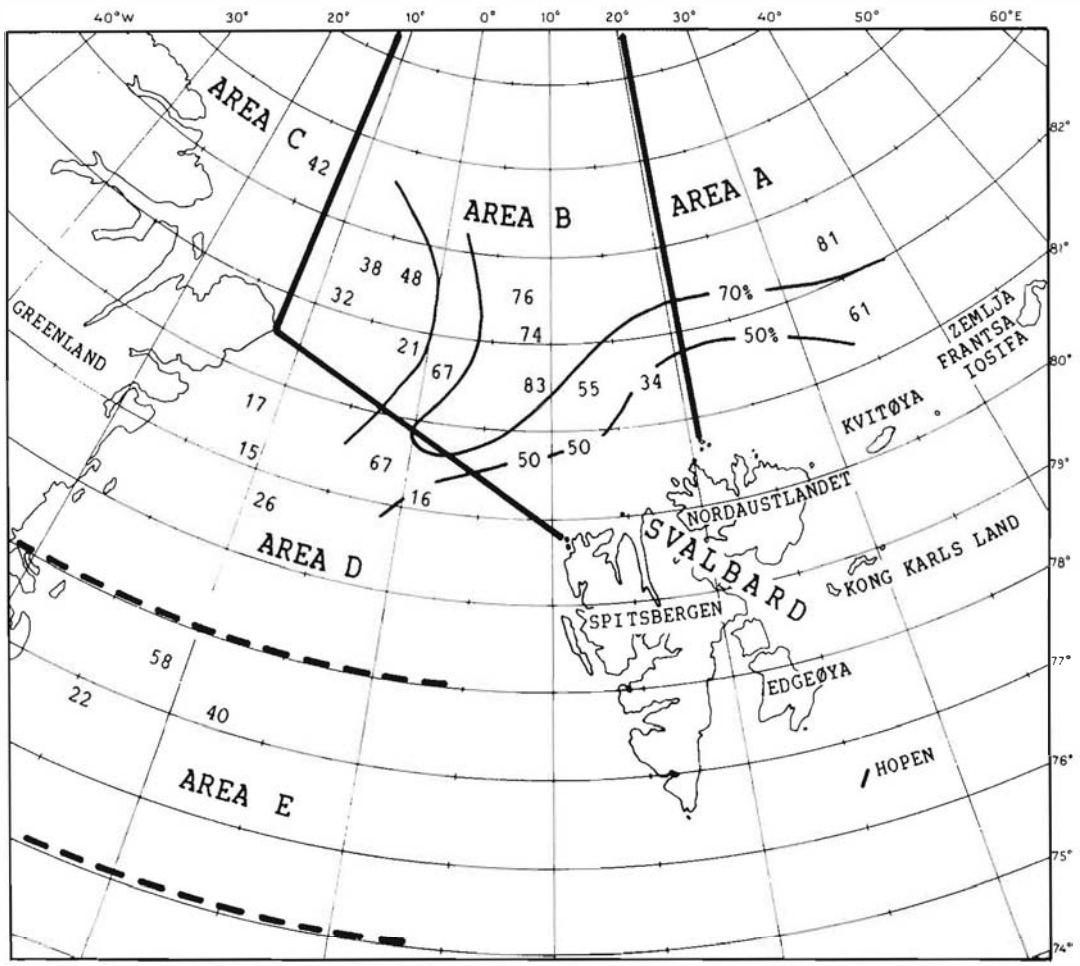

Fig. 11. The distribution of squared correlation coefficients for the meridional components of ice drift and geostrophic wind speeds. Only periods with buoy-days > 25 and a standard deviation of the geostrophic wind speed > 5 m s^{-1} have been used. The confined areas A, B, C, D referred to in the text are also given.

1982. There is, however, a marked change in the correlation for zonal movements from the first year to the second. Because the approximate linear relationship between the geostrophic wind and the ice drift does not hold for smaller wind speed, (e.g. Thorndike & Colony 1982), the difference in the standard deviation in velocity of the geostrophic wind (Fig. 12) would suggest a higher correlation for 1981 as compared with the 1982 results. Such an effect is also revealed by Table 3, i.e. small wind speeds correspond generally with a small correlation. For example, the smallest correlation (0.13) for buoy ID 1905 in area D in 1979 was obtained during a period when calm conditions prevailed for 50% of the time.

The wind factor A and the angle between the geostrophic wind (**G**) and the ice drift (**U**), the turning angle α, are determined for buoy drifts within the five confined areas from the relationship

$$\mathbf{U} - \bar{\mathbf{u}} = A(\mathbf{G} - \bar{\mathbf{g}}) \tag{5}$$

where $\bar{\mathbf{u}}$ and $\bar{\mathbf{g}}$ are the average ice drift and geostrophic wind vectors, respectively. There are some general features which can be observed. Apart from the special ridging area near Nord-

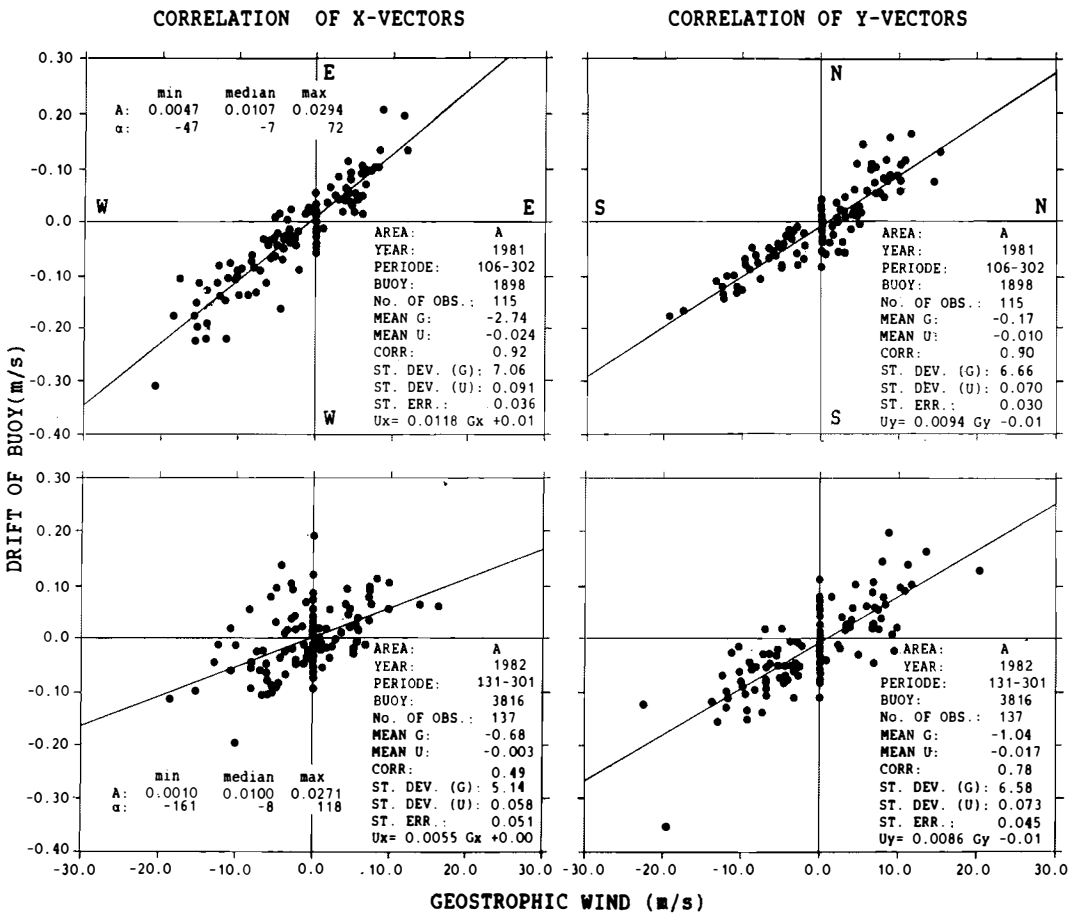

Fig. 12. Examples of regression analysis in area A, north of the Barents Sea for buoy drifts in 1981 and in 1982 as calculated from Equation (1).

ostrundingen, in parentheses in Table 3, the geostrophic wind factor varies between 0.007 and 0.013 in area B, north of the Fram Strait. This marked variation is probably due to the variable, constrictive effects which the passage exerts on the southbound ice drift stream. The seasonal variations of A and α in the central part of the Arctic Ocean are according to Thorndike & Colony (1982), 0.0077 and −5° for winter and spring, 0.0105 and −18° for the summer, and 0.0080 and −6° for the autumn seasons. These values are comparable with our all-season averages in area B, north of the Fram Strait, 0.0105 and −9°, respectively.

Table 3. — The mean meridional components (m s^{-1}, and positive southwards) of the ice drift U_y, the geostrophic wind G_y, the corresponding standard deviations σU_y and σG_y, the constant current c_y, and the correlation coefficient R as calculated from Equation (1) together with the geostrophic wind factor A × 10^3 and the turning angle α as calculated from Equation (5). N gives the number of buoy days. The relative importance of the currents for the total ice drift is indicated by c/U in the last row.

ID	N	Area	U_y	σU_y	G_y	σG_y	c_y	A×10^3	α	R×10^2	c/U
1976											
6044	10	B	0.051	0.063	−0.7	4.5	0.058	9	− 3	71	1.09
6236	20	B	0.088	0.073	1.2	6.0	0.080	12	−13	57	0.91
6236	48	D	0.071	0.141	1.1	7.1	0.062	19	−26	40	0.88
6072	48	D	0.034	0.111	3.3	9.4	0.020	10	+10	39	0.95
6044	14	D	0.087	0.069	1.0	6.2	0.081	13	− 3	54	0.94
6200	20	D	0.142	0.077	1.4	6.6	0.129	11	− 9	82	0.86
6200	33	E	0.072	0.107	0.1	5.7	0.072	23	− 4	63	1.07
1977											
7013	30	B	0.046	0.055	5.1	6.5	0.015	11	−30	71	0.51
7323	16	B	0.094	0.072	6.2	4.7	0.046	11	−11	49	0.57
7013	16	D	0.055	0.070	5.1	5.9	0.014	8	− 3	68	0.48
7323	17	D	0.107	0.101	4.8	7.4	0.050	12	− 4	86	0.59
7323	12	E	0.148	0.082	2.9	6.2	0.122	13	−44	68	0.78
1978											
8200	50	B	0.027	0.070	0.5	6.0	0.022	12	− 6	82	0.89
8236	16	B	0.096	0.105	1.2	7.1	0.082	11	− 3	79	0.89
8072	54	B	0.041	0.083	0.8	5.9	0.034	10	− 5	62	0.79
8072	7	D	0.061	0.089	0.7	5.0	0.053	17	−13	73	0.92
8236	36	D	0.063	0.068	1.8	4.8	0.050	12	+11	52	0.73
1979											
1593	74	B	0.049	0.093	1.7	5.6	0.029	12	− 8	74	0.59
1594	43	B	0.083	0.081	4.1	6.1	0.044	11	−11	71	0.51
1905	28	B	0.063	0.072	3.0	5.9	0.032	13	−17	86	0.51
1594	28	D	0.115	0.133	1.9	4.4	0.066	20	+ 5	84	0.58
1905	26	D	0.099	0.071	−0.1	3.0	0.099	14	− 7	13	1.01
1593	45	D	0.024	0.109	2.0	7.1	0.012	9	+14	42	0.38
1594	15	E	0.118	0.130	2.4	8.9	0.099	14	−19	55	0.73
1924	20	E	0.151	0.107	5.2	4.8	0.102	7	+25	43	0.68
1905	53	E	0.047	0.130	0.5	6.3	0.038	16	−13	76	0.80
1980											
1915	12	A	−0.030	0.076	7.0	6.9	0.011	9	+ 9	54	0.62
1915	67	B	0.025	0.081	0.1	9.5	0.025	8	0	58	1.00
1926	22	B	0.093	0.087	1.9	9.4	0.085	7	+21	46	0.90
1926	17	D	0.146	0.139	0.9	10.4	0.143	6	+39	23	0.99
1926	14	E	0.138	0.254	−1.9	12.0	0.172	18	+ 1	82	1.18
1981											
1898	119	A	0.010	0.069	0.2	6.6	0.008	11	− 7	90	0.46
1899	19	B	0.041	0.102	−0.3	5.3	0.044	(15	− 9)	60	0.96
1900	46	B	0.057	0.082	1.3	8.7	0.046	7	− 5	87	0.74
1899	48	C	0.032	0.053	4.5	6.7	0.009	5	−18	65	0.73
1899	19	D	0.155	0.095	−3.3	4.7	0.192	17	−12	55	1.24
1899	16	E	0.185	0.154	0.5	8.1	0.177	18	−20	76	0.88
1900	6	E	0.242	0.137	3.8	7.8	0.183	21	0	88	0.81
1982											
3816	164	A	0.017	0.079	0.3	6.9	0.008	10	− 8	84	0.98
3815	37	B	0.063	0.049	2.0	4.2	0.049	7	−14	59	0.82

Table 3, continued

3817	27	B	0.058	0.057	0.1	4.3	0.058	(7	+ 8)	26	1.02
3816	33	B	0.062	0.101	3.4	11.6	0.034	10	— 2	91	0.32
3817	57	C	0.027	0.038	1.4	4.1	0.022	5	—32	34	0.88
3815	21	D	0.134	0.103	0.7	5.7	0.128	5	+36	48	0.96
3817	33	D	0.096	0.079	3.7	5.6	0.062	9	+17	63	0.66
3817	11	E	0.091	0.054	3.6	4.6	0.067	9	0	57	0.67
1983											
3844	35	A	0.021	0.062	— 0.9	4.5	0.028	10	— 9	58	0.82
3844	23	B	0.108	0.051	8.0	5.2	0.049	9	— 7	74	0.42
3842	53	C	0.027	0.052	1.6	4.7	0.015	8	+12	69	0.68
3842	16	D	0.166	0.065	9.8	4.8	0.079	9	+ 3	66	0.47
3816	5	D	0.563	0.075	8.5	5.2	0.477	10	+46	70	0.87
3842	22	E	0.118	0.093	3.8	7.3	0.095	7	+10	47	0.76
3816	8	E	0.452	0.177	15.8	5.4	0.272	5	+26	35	0.62

The average wind factor changes from about 0.010 to about 0.020 when moving from the Arctic Ocean into the marginal sea ice zone in the Greenland Sea (Fig. 13). This spatial variation illustrates the increasing effect of the wind on the ice drift due to the increased divergence and the reduced internal stress gradients when the ice slips out from the Arctic Ocean. The wind factor observed in the marginal ice zone south of the Fram Strait is comparable with the wind factor estimated for ice edge displacements in the Barents Sea (Vinje 1977). From the marginal ice zone towards the Greenland coast, the wind factor reduces from about 0.020—0.023 to 0.007—0.009. This lateral variation is comparable with the observations made by Johannessen et al. (1983) across the marginal sea ice zone north of Svalbard in September 1979.

The annual average march of the meridional, geostrophic wind component in the Fram Strait indicates a net southward wind transport for all months, except August when the wind transport is at a minimum and directed northwards (Table 4). There is a marked annual variation of the local wind forcing with a relatively steep increase in a southwardly directed wind stress during the autumn as compared with the relatively slow abatement towards the minimum in August.

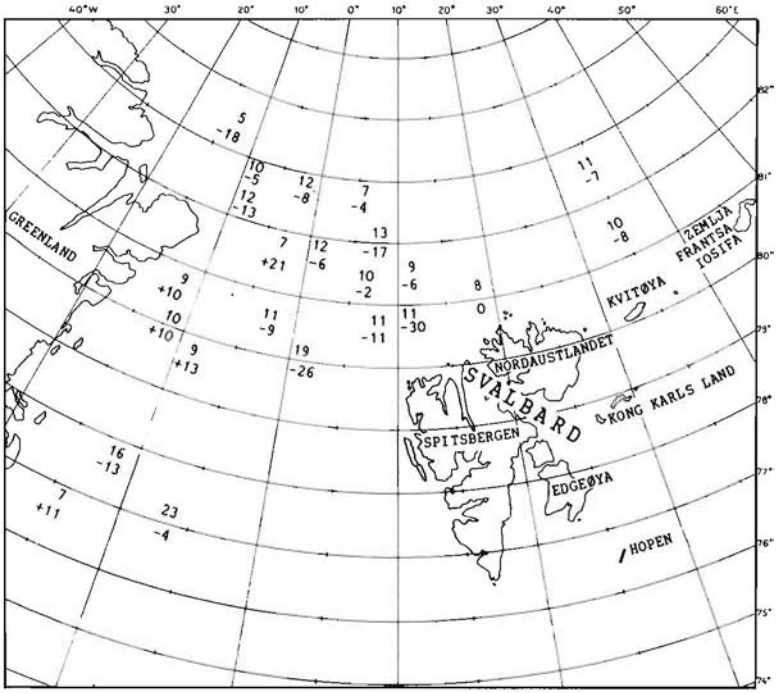

Fig. 13. The geostrophic wind factor A × 10^3 (upper number) and the turning angle α (lower number) as calculated from Equation (5) for periods with more than 25 buoy-days and a standard deviation of the geostrophic wind speed greater than 5 m s^{-1}.

Table 4. — Monthly average southward (+) ice drift speed (A × Gy), cm s^{-1}, as induced by the local meridional geostrophic wind speed component (Gy) in the Fram Strait, 1976—1984. The applied geostrophic wind factor, A = 0.0105, is the average observed just north of the narrowest part of the Strait.

Wind drift, cm s^{-1}												
Jan	Feb	Mar	Apr	May	June	Jul	Aug	Sep	Oct	Nov	Dec	Year
3.5	2.3	1.5	2.0	0.9	1.3	0.4	—0.2	2.2	1.6	3.7	2.2	1.8

The annual average ice drift speed through the Fram Strait as induced by the local wind stress field is, accordingly, only 0.018 m s^{-1}. This is a small value as compared with the cross-strait average of the ice drift speed which, at 81° N, is 0.079 m s^{-1} (Table 2). This comparison suggests that the current-induced ice drift on an average accounts for about 77% of the total ice drift at the 81st parallel in the Fram Strait. This figure will be discussed in greater detail in the next section.

2.1.2. Current drift. — Felzenbaum (1958) shows that the percentage share of the current drift, as part of the total ice drift, increased from 50 to 80% as the North Pole 2 station drifted from the central part of the Arctic Ocean towards the Fram Strait. Doronin & Kheisin (1975), investigating the time dependency, report on average percentage shares of 15, 20, 33 and 52 for 1, 10, 30 and 365 days, respectively, for this manned station. Thorndike & Colony (1982) also report on a percentage share of 50 in the central Arctic Ocean when considering periods of several months. On shorter time scales and in all seasons they find that this percentage share is reduced to about 30. In accordance with the results of Felzenbaum on the spatial dependency, our buoy observations show that the ocean currents in about 65% of the periods considered contribute to more than 70% of the total ice drift through the Fram Strait (Table 3). The average values for the various areas indicate that the mentioned percentage share increases from 75 in area B, through 79 in area D, to 82 in area E, revealing an increasing current transport as the ice passes from the Arctic Ocean into the Greenland Sea.

However, comparing c/U given in Table 3 with the residence time, which varies between one and eleven weeks, a scatter diagram shows no discernible increase of this percentage with time, as has been observed in the Arctic Ocean. This result seems reasonable because the wind effects transferred to the ocean locally in the Fram Strait will here be advected out of the area far more rapidly than is the case for a given area in the Arctic Ocean.

The calculated mean surface current shows great temporal and spatial variations (Figs. 14 and 15). The variability is particularely large in area D, just south of the narrowest part of the Strait. Aagaard & Coachman (1968) estimated the total transport in the East Greenland Current (EGC) based on measurements from the ice island ARLIS II when it drifted along the eastern coast of Greenland in 1965. Aagaard (1970) also gives the annual integrated Sverdrup transport in the Norwegian-Greenland Sea for the same year, and he obtained a fair agreement between the two different methods with regard to the volume transport of the EGC. Aagaard studied the current transport south of 78° N, i.e. south of the Fram Strait. However, when the EGC is speeded up further south due to an increased regional atmospheric circulation one should expect, from continuity reasons alone, that this will in turn affect the currents in the Fram Strait as well. This means that the drift speed of the ice transported by the Transpolar Current towards the passage between Greenland and Svalbard should also here be influenced by lagged effects caused by the wind stress field further south in

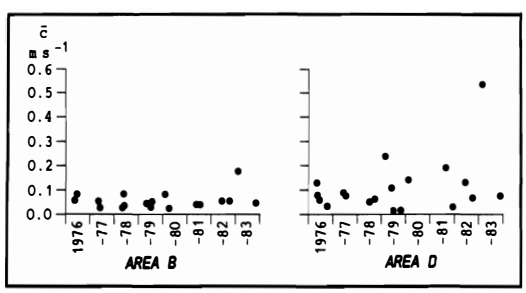

Fig. 14. The temporal variation of the non wind induced ice drift, here referred to as the mean surface current c, calculated from Equation (1). Numerical values given in Table 2.

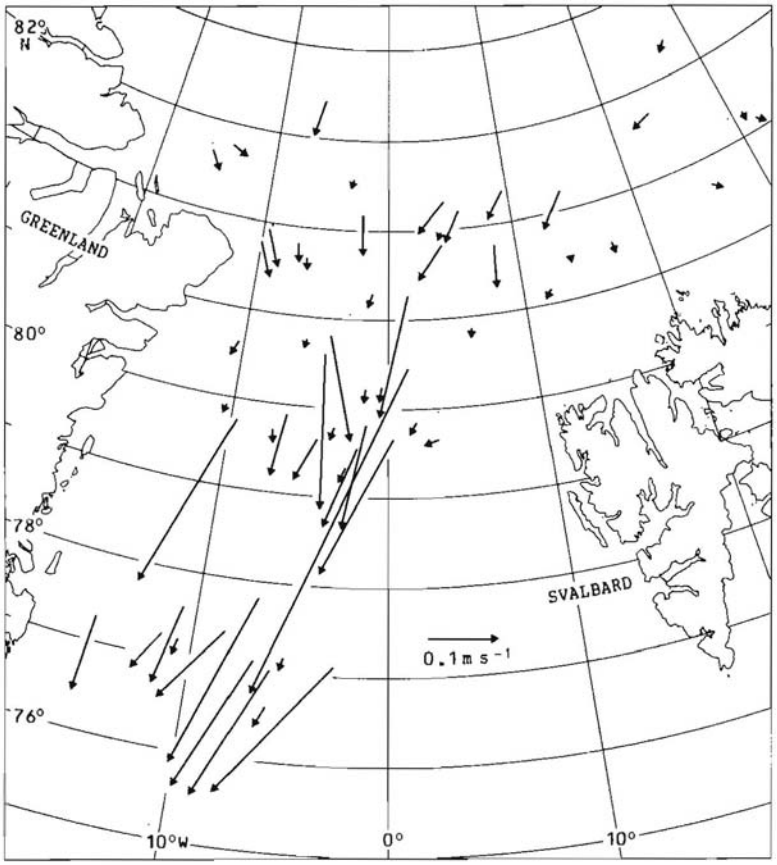

Fig. 15. Spatial variation of the average surface current as calculated from Equation (1).

the Norwegian and Greenland Seas. Such a connection is clearly illustrated by the corresponding increase of the ice drift speed in the Strait, and the air pressure differences between the Strait and the central area of the Greenland-Norwegian Seas as provided in Table 2.

The long term continuity constraints mentioned above should cause corresponding long-term variations in the surface currents in the Fram Strait. In addition, we should also expect short term variations to occur in correspondence to the geostrophic adjustment necessary to compensate for the variable, wind-induced transport of surface water perpendicular to the coast of Greenland. The latter effect is illustrated by the marked dependency found between the current speed and the cross-current wind speed, as calculated for the buoy drifts in the central core of the ice drift stream (Fig. 16A).

A regression analysis of the relationship between the surface current calculated from Equation (1) and the cross-current geostrophic wind speed component also suggests a marked increase of the correlation with increasing time-lag (Fig. 16B), indicating a maximum after about one week. This may suggest the time scale for a primary geostrophic adjustment. An extension of the correlation beyond about one week time lag results in a fluctuating correlation coefficient, possibly reflecting the integrated effects of passing lows.

Our calculations suggest also an increasing correlation with increasing cross-coastal wind speed and this seems reasonable (Fig. 16B). Similar correlation studies for the buoys drifting over the shelf area give no systematic increase of the correlation with increasing time lag. This may possibly be due to the predominance of the back-water circulation in that area.

It is of interest to note that an increased cyclo-

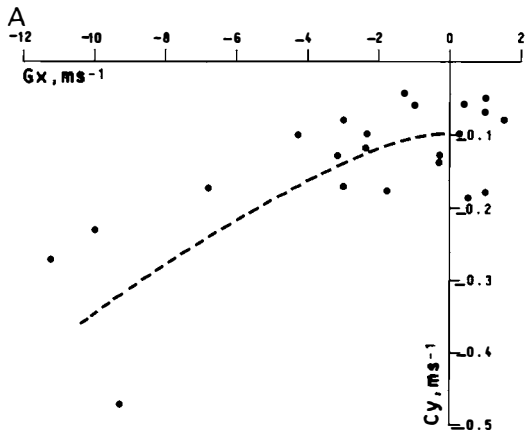

Fig. 16. A. Relationship between the calculated meridional surface current component (C_y, negative southwards) and the cross-stream geostrophic wind speed component (G_x, negative westwards) both given in m s^{-1}, for selected buoy drifts along the shelf break in areas D and E (cf, Table 3).

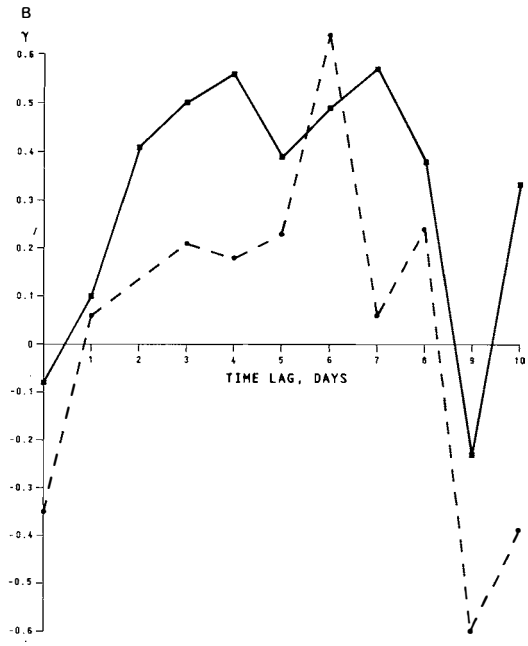

B. The time lagged correlation between the surface current speed and the corresponding cross-current geostrophic wind speed for the buoys 1900 (——) and 3815 (- - - -) which passed in the central part of the Fram Strait. The mean cross-current geostrophic winds are from the east with speeds of 2.1 and 0.5 m s^{-1}, respectively.

nic activity in the Norwegian-Greenland Sea also seems to produce a special sea ice distribution in the area (Vinje 1980). Very pronounced developments of the features Odden and Nordbukta - visualizing the oceanic circulation in the Greenland Sea Gyre — correlate with prevailing subnormal air pressures in the Norwegian Sea. An example is given in Fig. 17. Increased cyclonic activity between Greenland and Scandinavia may accordingly cause an increased efflux of ice from the Arctic Ocean together with an increased cyclonic circulation in the Greenland Sea Gyre.

Correlating the average speed, Umax, of fourteen drifts in the main core of the ice stream across the 81st parallel with the one week lagged pressure difference, ΔP, between 81° N, 15° W and 73° N, 5° E (Fig. 18) we get the regression equation

$$(6) \qquad \text{Umax} = 0.095 + 0.00635\Delta P(\text{m s}^{-1})$$

where the standard error of estimate of Umax on ΔP is 0.039 m s^{-1} and the correlation coefficient is 0.72. The air pressure difference, ΔP, has been obtained from the European Meteorological Bulletin, Deutscher Wetterdienst. The squared correlation shows that about 50% of the variation of the ice drift speed in the central part of the Fram Strait can be explained by variation in the air pressure distribution in the Norwegian-Greenland Sea.

The weighting function given in Fig. 10 and the above relationship will subsequently be used for an estimate of the seasonal variation and the monthly range of the export of ice.

Applying the geostrophic wind factor (A) and the turning angle (α) for the various periods and areas considered (Table 3), the daily current, based on daily values of ice drift and geostrophic wind speed, has been calculated according to Equation (1). The mean pattern is given in Fig. 19. The calculated surface currents suggest a slow backwater circulation in the area north of the Barents Sea, probably reflecting a branching of the Transpolar Current. This indicates that there

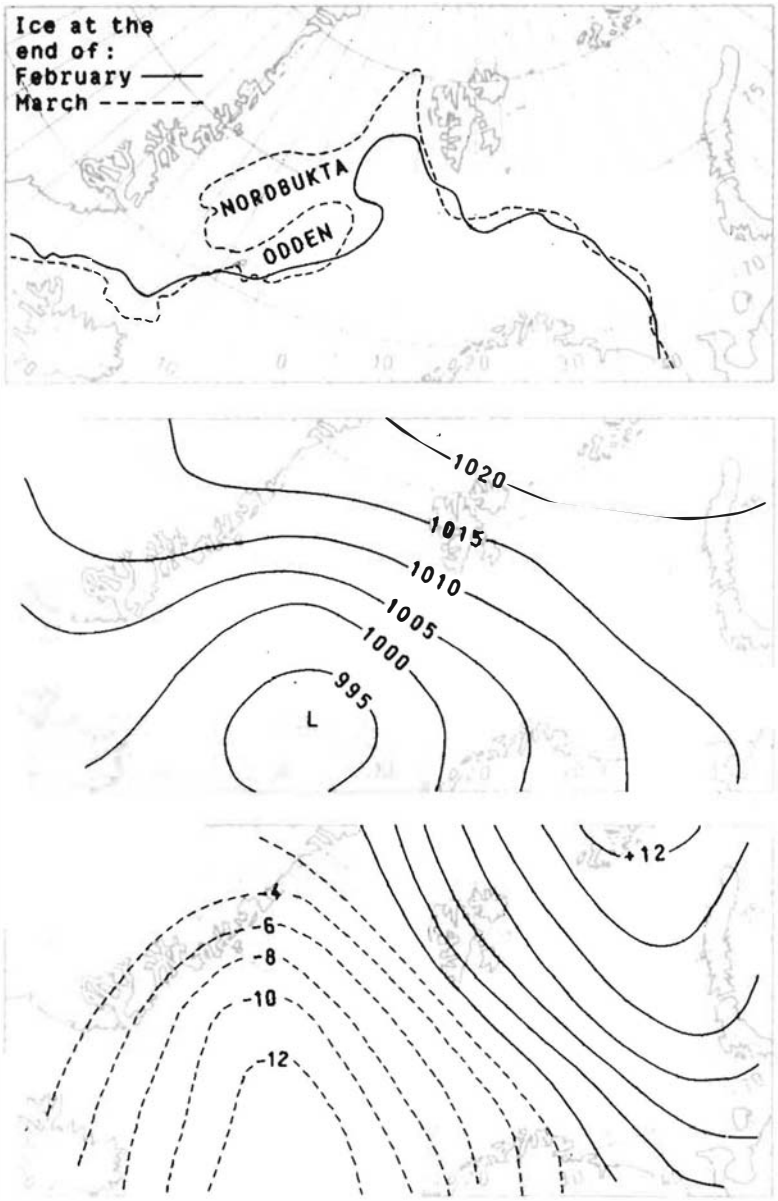

Fig. 17. An especially pronounced development of the ice distribution in the Greenland Sea Gyre which envolved from the end of February towards the end of March 1979, and the contemporary mean atmospheric circulation and the deviation (mb) from the long term means.

is a small net influence on the ice drift by currents and that the main forcing is caused by the wind stress field in this region. In this connection it can be mentioned that Zacharov (1976) and Vinje (1986) show that the Barents Sea may be a net ice source for the Arctic Ocean over periods of a decade or more.

We observed a local minimum of the ice drift speed at 80° N and 2—5° E (Fig. 8). A similar minimum is also seen in the average surface currents (Fig. 19). This is in accordance with the fact that the ice edge in this area has a very stationary position. Further south the maximum zone of the calculated surface current is seen to follow the

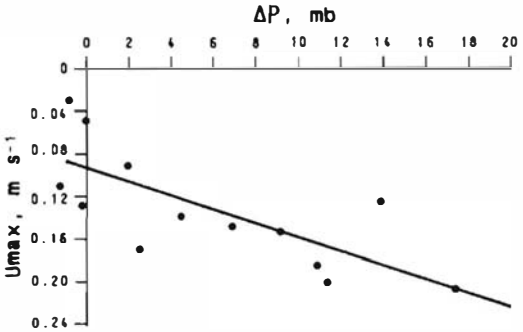

Fig. 18. The relationship between meridional drift speed observations in the central core of the ice drift stream between four and ten degrees W at 81° N, and the corresponding air pressure difference between the Fram Strait (81° N, 15° W) and the central area of the Norwegian-Greenland Sea (73° N, 5° E). In accordance with the suggested increase in correlation discussed above (Fig. 16B), the air pressure readings have been made one week in advance of the drift observations.

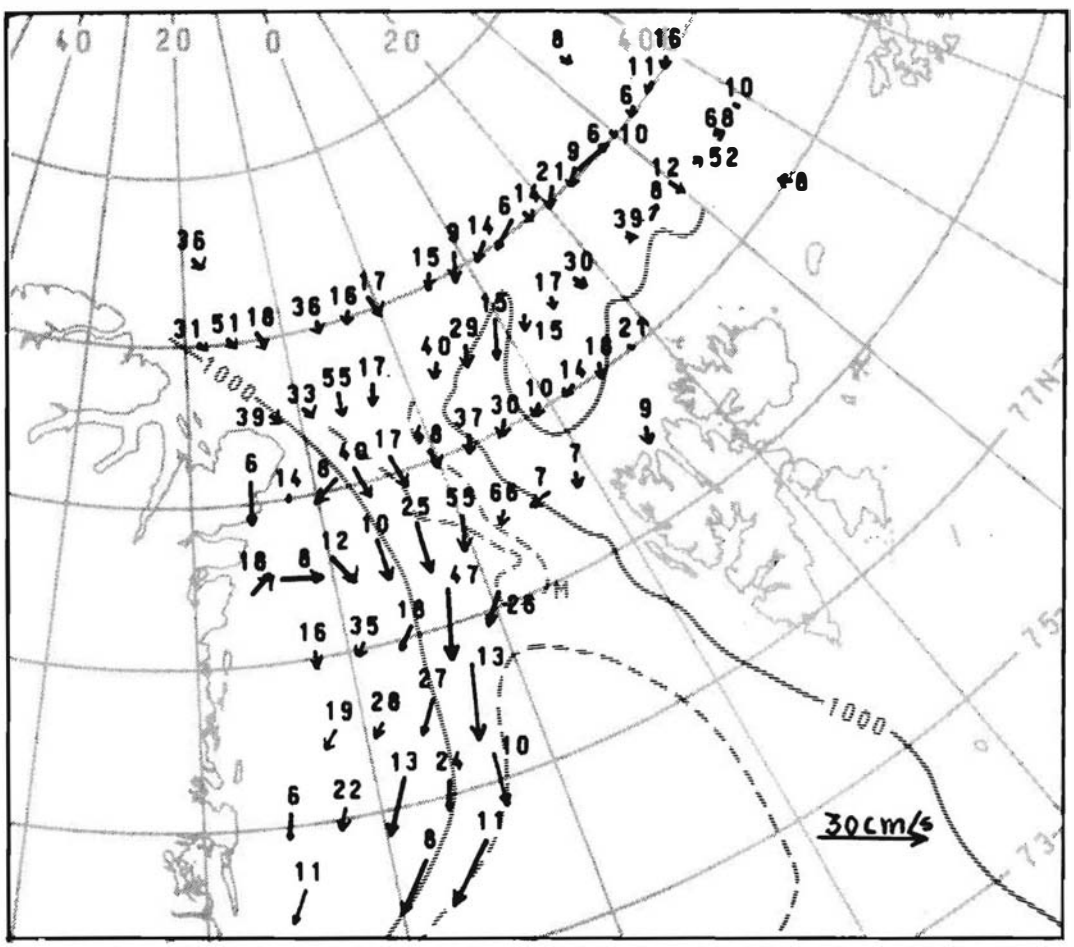

Fig. 19. The pattern of the calculated surface current, based on daily values. The daily values have been determined from Equation (1) by applying the appropriate constants estimated for the various confined areas and using the daily observed values of U and G.

continental shelf break. There is some indication of a small branching of this maximum zone near 77° N. This is also observed in the ice drift pattern (Fig. 8). Otherwise the maximum zone of the surface current seems to be narrower than the corresponding ice drift maximum along the shelf break. This could possibly be explained by a lateral dispersion of water stress momentum caused by the varying direction of the local wind forcing.

2.2. Ice thickness distribution

2.2.1. Submarine observations. — The first ice thickness information from the Fram Strait is based on upward-looking sonar profiles obtained from American and British submarines. The British observations are discussed in detail by Wadhams (1981a, 1983) and the American observations are given as isolines by Hibler (1980). The

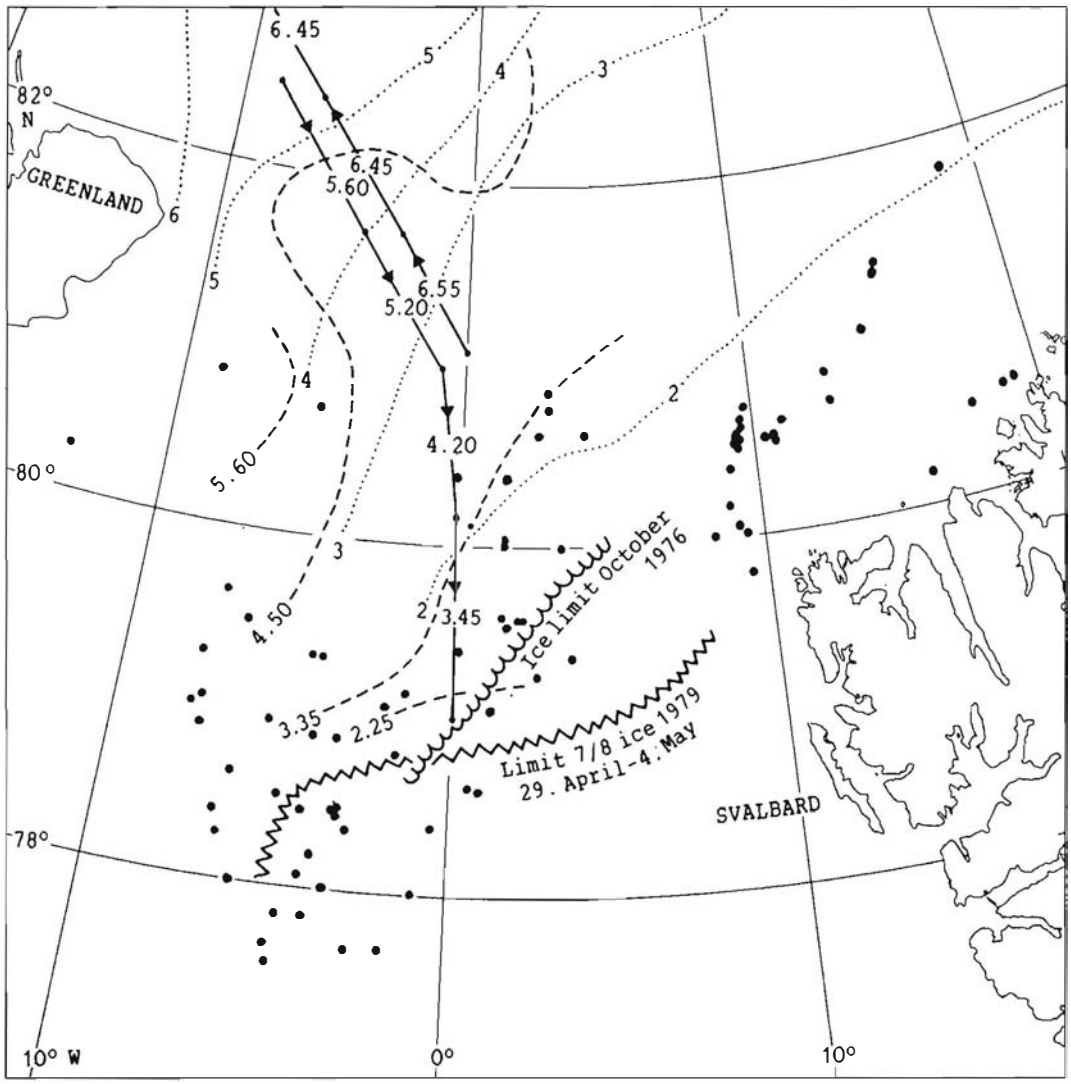

Fig. 20. Submarine observations after Hibler (1980) ...., Wadhams (1981) ———, and (1983) - - - -, and the ice drilling sites.

observations reveal a considerable cross-stream variation of the ice thickness, from 1—2 m in the marginal areas to 5—6 m when approacing the Greenland shelf (Fig. 20). The first submarine observations were made in October 1976 (Wadhams 1981a). The observations show ice thicknesses which are in considerable excess compared with observations obtained during the spring (1977 and 1979), as well as compared with the drillings made during July and August 1981—1984, discussed below.

Based on statistical calculations Rothrock (1981) considers a 100 km submarine sonar profile to have an uncertainty of ±0.2—0.4 m, which may be critical for thin ice estimates. Wadhams (1981a) takes it to be zero with random means. Another error is caused by the smoothing of the surface by the sonar beam. A correction factor for this effect was calculated by Wadhams (1981a) from a comparison between distances measured by narrow- (h_n) and broad-beam (h_b) upward-looking sonars. The comparison shows that the percentage correction of the mean observed draft is 16%. This comparison is, however, only strictly valid over the range $3.2 < h_n < 4.7$ m, and in this interval only 5% of the uncorrected submarine observations (h_b) for 1976 are contained. The interpretation of the results as calculated this year for observations outside the above interval should, therefore, be made with caution (Wadhams 1981a). In this connection it is noted that the comparison with the surface laser profile along the submarine track gives a buoyancy factor (thickness of ice below/above the water surface) of 8.35 (Wadhams 1981a). The drillings discussed below give the somewhat lower ratio of 7.35. This discrepancy suggests that the submarine observations provide an overestimate of keel depths for the more heavier ice. Wadhams' caution, and the latter comparison therefore, lead ut to refrain from using the 1976 submarine observations in a later estimates of an average ice thickness in the Strait.

2.2.2. Cross-stream ice type variation. — A cross-stream variation of the ice thickness as observed from the submarines agrees with the drift pattern in the Arctic Ocean as given by Vize (1937), Gordienko (1958), Zacharov (1976), and by Colony & Thorndike (1983). The thinner ice in the eastern part of the ice stream comes mainly from the seasonal sea ice zones over the Siberian shelves, the Kara and the Barents Seas while the thicker ice in the western part comes mainly from the Beaufort Sea and from the strongly ridged areas north of Greenland.

There is a variable transfer of ice from the Beaufort Sea to the Transpolar Ice Drift Stream (Volkov & Gudkovic 1967; Strübing 1968), and this will eventually give rise to a temporal variation in the ice thickness distribution in the Fram Strait. The mean relative distribution of the various ice types observed during our five crossings of the Fram Strait is shown in Table 5.

Table 5. — Percentage coverage of various ice types and deformed ice in the Fram Strait based on observations from LANCE in July-August 1981—1984 and from POLARSTERN in July 1984. Observations are made at the drilling locations given in Fig. 20.

	West		East	
	10—5	5—0	0—5	5—10
Multi-year ice	78	57	32	26
Second-year ice	8	36	43	55
Winter ice	14	7	25	19
Deformed ice	29	25	27	19

The observed distribution of multi-year ice, second-year ice, and winter ice is in accordance with the above picture of the origin of the ice passing the Fram Strait. It is noted that the ridging in the marginal ice zone, 5° — 10° E, is somewhat less than the ridging further west. This is to be expected because of the greater possibility for a redistribution after ridging has taken place, as well as the more intense disintegration in the marginal areas both due to melting and mechanical wave action. Submarine observations in April—May 1979 (Wadhams 1983) show a clear difference in keel densities between the marginal ice zone (0.5 keels per km track), and the more interior or northern areas in the Fram Strait region (1.8—2.9 keels per km track). Wadhams concludes that the ridging in the latter area is characteristic of Arctic Ocean interior ice.

Again we observe (Table 5) an indication of the effect of the freezing processes in the Nordostrundingen polynya, suggested by the increased concentration of winter ice when approaching this area. Evidence of the melting effect of the warm West Spitsbergen current is provided by

the relatively low percentage of winter ice in the eastern part of the Fram Strait.

Our field observations show that about 85% of the ice flow, on an average, consists of multi-year and second-year ice (Table 5). This is in great contrast to the corresponding concentration of about 50% which Kloster & Svendsen (1982) and Svendsen et al. (1983) obtained for the ice conditions in September-October 1979 when applying the NORSEX algorithm for the interpretation of NIMBUS-7 SMMR data in this area. Cavalieri et al. (1986), applying an algorithm based on the dual-polarized multispectral radiance, obtained a still lower percentage coverage of multi-year ice in this area for the period 3—7 February 1979. It seems unrealistic to ascribe the marked discrepancy to interannual variations. The comparison may therefore reflect some of the significant uncertainties which according to Cavalieri et al. (1986) still exist with regard to the determination of the fraction of multi-year ice from the NIMBUS-7 SMMR data.

2.2.3. Drillings. — Ice thickness measurements in the Fram Strait were made from LANCE in July—August, 1981—1984, and in July 1984 also from POLARSTERN both by drilling and by measurement of surface of fractures. Altogether 382 drillings have been made on level ice at reasonable distances from ridges in the various areas as given in Fig. 20. The Markov-Wittman model (Wittman & Schule 1966) has been used as a guideline. This model suggests that the subsurface horizontal extension of a ridge is one order of magnitude wider than the surface extension.

Although the ice field as a whole seems to be in isostatic equilibrium, pronounced local deviations from isostasy seem to be common (Fig. 21). This is in accordance with previous observations by e.g. Yakovlev (1955), Bushuev (1966), Nazincev (1971), and Hibler et al. (1972). When determining the linear regression between the thickness T and the freeboard F, we note that these two dimensions are highly dependent variables. This means that we cannot apply the usual approach in curve-fitting by minimizing the ordinate- or abscissa-deviations from the regression line. We have therefore forced the regression line through origin. We obtain

$$T = (8.35 \pm 0.11)F \quad (7)$$

or

$$D = (7.35 \pm 0.11)F \quad (8)$$

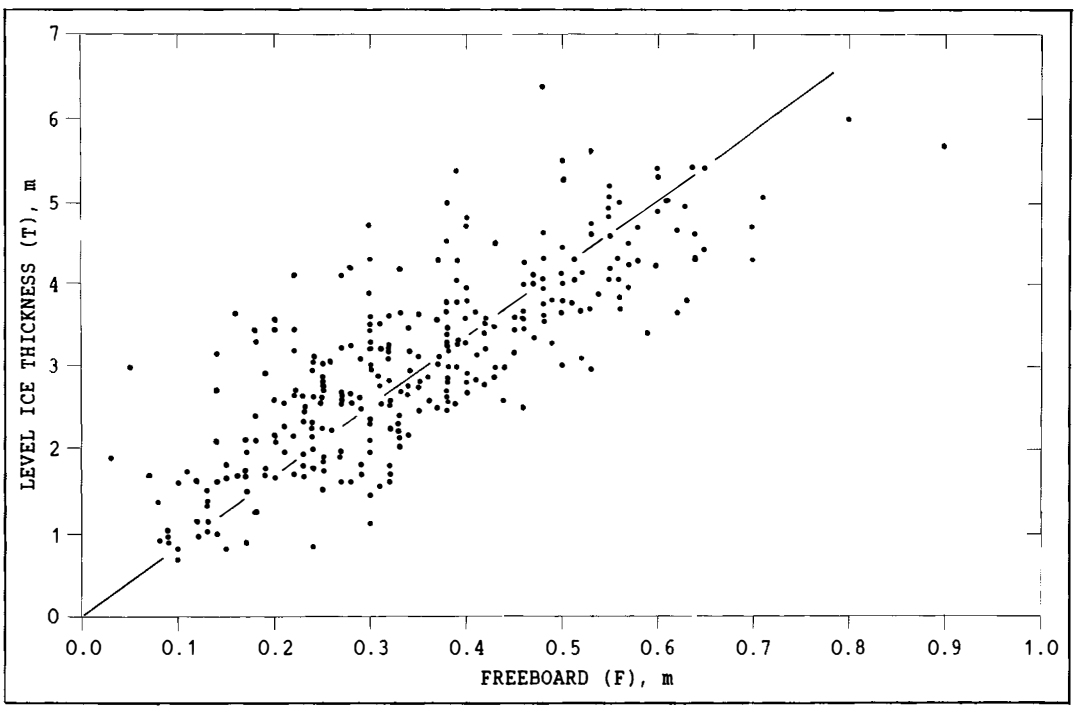

Fig. 21. Ice thickness versus freeboard of level ice in the Fram Strait.

where $D = T - F$ is the ice draft. The correlation coefficient is 0.80 and the standard error of estimate of T on F is 0.68 m. Assuming a sea water density of 1030 kg m^{-3} we arrive at an average sea ice density of 907 kg m^{-3} which is comparable with 910 kg m^{-3} measured from ice cores in the Beaufort Sea (Hibler et al. 1972) and with the calculated density of 921 kg m^{-3} as determined from 110 drillings on the drifting station NORTH POLE 13 (Nazincev 1971). Hibler et al. (1972) further obtained the ratio of $T/F = 8.58$ with a correlation coefficient of 0.79 and a standard error of estimate of T on F of 0.60 m, in fair accordance with our measurements.

There are, however, some considerable discrepancies when comparison is made with Hibler et al.'s (1972) measurements and with the results represented in Fig. 3 in Ackley et al. (1974). Hibler et al. determined the relationship

$$H = 2.32\,F + 2.80\,(m)$$

from 31 drillings on a multiyear ice floe in the Beaufort Sea. In calculating the regression line, the freeboard — corrected for the influence of the snow depth — was taken as the free variable. The analogous result for the Fram Strait data gives

$$H = 6.09\,F + 0.95\,(m)$$

which differs markedly from the former relationship. Although the two drilling series are taken at different times of the year, the marked discrepancy in the results at the two locations are unexpected. It is supposed that this is, at least partly, due to the different extension of the areas considered, as well as the number of observations.

A number of drillings were made through a varying number of ice floes at each site (Fig. 20). The thickness of the thinner ice in the drilling area was determined either by measuring the fractures against a known length marked on the rail of the vessel, or by age determination. The average ice thickness representative for a given location has been obtained by weighting the relative percentage coverage of the various ice types in the area.

Our drillings and measurements of surfaces of fractures should give a fair estimate of the average thickness distribution of level ice across the Fram Strait. To obtain the total mass, a correction for ridging has to be made. Hibler et al. (1974) give the following formula for the equivalent thickness of ridged ice,

$$h_r = 10\,\pi\,\mu\,(h_S)^2 \qquad (9)$$

where μ is the number of ridges per kilometre above height h, and $(h_S)^2$ is the mean square sail height of ridges higher than h, which is called the cutoff height. Leppäranta (1981) suggests a formula for the equivalent thickness of the deformed ice with ridge heights less than h, here denoted $h_d{}'$

$$h_d{}' = h_r(1 - h/h_S)\exp(h/(h_S - h) - 1) \qquad (10)$$

Palosuo & Leppäranta (1982) use equations (9) and (10) to estimate the total ice mass based on laser profilometry of ridges from YMER north of Svalbard and Frans Josef Land (Table 6).

Based on comprehensive laser profiling over the western part of the Arctic Ocean in 1970—1973, Hibler et al. (1974) give an average, weighted equivalent ice thickness of 0.5 m of deformed ice having sails above 0.61 m (cutoff height). Applying (9) and (10) these observations suggest that the deformed ice in the Fram Strait may, in total, add to the mean thickness of level ice with an equivalent of about 0.7 m (Table 6).

Table 6. — Equivalent ice thicknesses of deformed ice north of Svalbard (Sv) and in the western part of the Arctic Ocean (AO), as estimated by Palosuo & Leppäranta (1982) and Hibler et al. (1974), respectively.

Area	Equivalent ice thickness, m. Ridges	Cutoff height	Rest of deformed ice	Total
North of Sv	0.2	1.0	0.3	0.5
Western AO	0.5	0.6	0.2	0.7

The contribution to the average ice thickness caused by ridging north of Svalbard is for the cutoff height of 1 m less than that caused by the deformed ice with sail heights below 1 m. This seems reasonable, because the average of the total number of ridges (regardless of heights) has a median value around 10 km^{-1} in these areas

Table 7. — Ice thickness observations in the Fram Strait grouped with respect to longitude. The observations were collected during July and August 1981, 1982, 1983, and 1984. The equivalent thickness of the deformed ice has been taken from Table 6.

Longitude	No.of drilling sites	Level ice	St.dev.	Deformed ice	Total thickness
West					
10— 5	15	3.31	0.63	0.7	4.0
5— 0	28	3.70	0.93	0.7	4.4
East					
0— 5	18	2.92	1.00	0.7	3.6
5—10	14	2.81	0.59	0.5	3.3
10—20	14	2.42	0.85	0.5	2.9

Table 8. — Average thickness (m) of the total ice mass along the 81st parallel in the Fram Strait as estimated from surface observations (drillings and measurements of the surface of fractures) made during July—August 1981—1984 and from submarine draft observations in April—May 1979. The equivalent thickness of the deformed ice has been taken from Table 6.

	West		East		
Longitude	10—5	5—0	0—5	5—10	10—20
Surface obs.	4.4	4.4	3.6	3.3	2.9
Submarine obs.	4.7	4.5	3.7		
Weighted average	4.5	4.4	3.6	3.3	2.9

(Vinje 1985), and the corresponding number of ridges per kilometre is only 2 to 4 when considering heights above 1 m as has been done in the table above.

The ice thickness measurements in the Fram Strait together with the equivalent thickness of ridged ice is given in Table 7.

As indicated by the large standard deviations, there is a great variability of the level ice thickness from place to place in the ice drift stream. The standard deviation is largest in the interval 5° W to 5° E. This span covers the central part of the ice stream as well as the longitudinal variation of the position of the ice edge zone (Vinje 1976, 1986). Therefore, the large standard deviation, to some extent, is affected by the longitudinal variation of the ice edge and is accordingly not representative for the ice that passes the measuring line, between 5° W and 5° E further north.

The observed lower ice thicknesses between 5° W and 10° W can probably be ascribed to the effect of locally formed winter ice in the Nordostrundingen polynya (Table 5). The winter ice observations in this interval will therefore be disregarded when calculating the thickness of the ice that comes from the Arctic Ocean. Hence, we produce the average of all observations made on multiyear ice for the longitudinal interval 10—5° W only. The equivalent thickness of ridged ice is kept unaltered, and is equal to 0.7 m. (Table 8). The average total ice thickness as observed from a submarine in April—May 1979 across the Fram Strait has been estimated from Fig. 1 in Wadhams' paper (1983) and is also listed in Table 8.

The thicknesses obtained by surface observations and corrected for ridging, are on average 17 cm less than the submarine observations. The surface observations have been made about two months before the minimum seasonal thickness is generally expected, while the submarine observations were performed during a period when maximum seasonal thicknesses should be expected. The afore-mentioned difference could therefore be explained by the seasonal variability. However, because of the different methods

applied, and an assumed interannual variation, the very good agreement which is indicated may be fortuitous.

According to our surface measurements the cross-strait ice thickness along the 81st parallel varies between 4.4 m near the coast of Greenland and 2.9 m at the northern tip of Svalbard. The relative importance of these thicknesses for the volume export varies with the corresponding drift speed and concentrations. When considering average values, we calculate a mean cross-strait weighted thickness of 4.0 m. Although the cross-strait average cannot straight away be considered as representative for an Arctic Ocean average, our figure can be compared with 3.7 m, which Koerner (1973) obtained as an ocean-wide mean thickness from a budget study. Considering the narrower ice stream further south, between Nordostrundingen and 79°N—0°W, Wadhams (1983) gives an average thickness of 4.06 m based on the 1979 submarine observations. All these values are substantially higher than 3 m, which has been the average thickness traditionally referred to in the literature.

The frequency distribution of the thickness of level ice (Fig. 22) reveals two distinct modes, one with a maximum at one metre, representing the winter level ice, and another with a maximum at 3 m, representing the multi-year level ice. The latter figure may be considered the most frequent thickness of level ice which has formed thermodynamically over several years in the Arctic Ocean. This figure, based on July and August observations, can be compared with the equilibrium ice thickness of 2.7 m which, according to the thermo-dynamic model of Maykut & Untersteiner (1971), should be reached two to three months later, at the end of October. Our observations are also in fair accordance with the level ice drafts measured from submarines in October 1976 in the Fram Strait (Wadhams 1981a) showing a frequency of level ice between 2.8 and 2.9 m (when corrected for the wide beam sonar averaging effect). Thus a fair agreement has been shown between theory, indirect and direct measurements with regard to the most frequent equilibrium thickness of the level multi-year ice which is transported out of the Arctic Ocean.

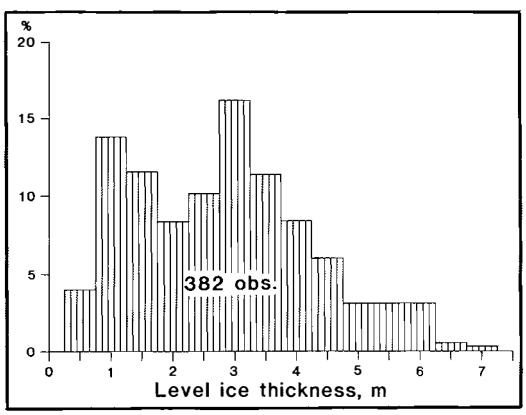

Fig. 22. Frequency distribution of level ice thickness.

A relatively high frequency of ice thicknesses between 5 and 6 m is observed. Ice of such a thickness may have originated from the area north of Greenland and from the Beaufort Sea. Part of the relatively high frequency exhibited may also be due to the fact that there is not always a correspondence between surface and subsurface features (e.g. Nazincev 1971).

2.3. Ice concentrations

The cross-stream sea ice concentrations have been determined from the weekly ice charts edited by the Norwegian Meteorological Institute and by the US Navy-NOAA Joint Ice Center, Suitland. The ice charts have been compiled from weather satellite images, and supported by observations from aircraft and ships during the summer season. The summary is represented in Table 9.

The influence of the strong, warm West Spitsbergen Current is clearly reflected in the annual variation of the ice distribution on the eastern side of the Strait. There is also a marked annual variation of the ice cover in and near the Nordostrundingen polynya revealing a marked minimum in the ice concentration at the end of August.

3. The ice volume transport

The ice volume transport can be calculated in two ways, either with the aid of Tables 2, 8 and 9 directly, or by substituting Table 2 with the introduction of an external parameter, the air

Table 9.— Ice concentrations in per cent along 81° N. The numbers give the average ice concentration at the end of each month for the period 1976 to 1984.

	West			East				
	12—10	10—5	5—0	0—5	5—10	10—15	15—21	Mean
Jan	100	100	100	100	100	100	100	100
Feb	98	99	99	100	100	98	98	98
Mar	99	100	100	100	100	100	100	100
Apr	88	98	98	98	98	98	92	97
May	80	86	96	96	96	93	90	93
Jun	56	77	98	98	86	86	67	85
Jul	77	74	81	89	91	74	53	77
Aug	46	51	76	79	72	63	39	63
Sep	76	84	97	89	83	71	39	77
Oct	87	97	97	90	87	81	70	87
Nov	91	94	97	94	87	72	72	86
Dec	89	97	99	98	86	86	86	92
Year	82	88	95	94	91	85	75	88

pressure gradient ΔP, which determines the ice drift speed by Equation (6). We shall first consider the more direct method.

It is clear that the rate of the volume export of ice through the Fram Strait should increase considerably from summer towards winter as all parameters involved act in the same direction (Tables 2, 8, and 9). The average rate of the meridional transport for the summer months May—August, 1976—1984, thus becomes 0.090 mill $m^3 s^{-1}$, while the average export during the period September—April turns out to be about twice as large, 0.193 mill. $m^3 s^{-1}$. The weighted annual average becomes 0.159 mill. $m^3 s^{-1}$, corresponding to 5000 km^3 of ice per year.

To obtain an estimate of the seasonal and interannual variation, we apply Equation (6) and Fig. 10 from which we estimate the monthly average drift speed profile as determined by the air pressure distribution in the Norwegian-Greenland Sea. When calculating the fluxes we then use the corresponding ice thickness (Table 8) and the observed ice concentration for the individual month. Again we find a considerable average seasonal variation, with a minimum in August of 0.079 mill. $m^3 s^{-1}$, and a maximum in January of 0.213 mill. $m^3 s^{-1}$ (Fig. 23).

The average annual export rate across the 81st parallel for the nine years considered becomes 0.154 mill. $m^3 s^{-1}$, corresponding to 4880 km^3 per

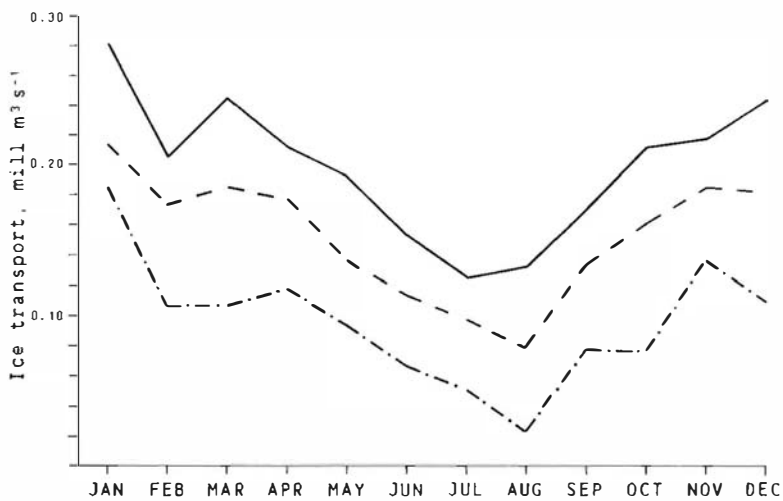

Fig. 23. The monthly mean, maximum, and minimum ice export for the period 1976—1984.

Table 10. —The mean annual meridional ice transport (1000 $m^3 s^{-1}$) within various latitudinal intervals in the Fram Strait, 1976 – 1984.

	West			East				
	12—10	10—5	5—0	0—5	5—10	10—15	15—21	Total
81°N	8.5	45.7	39.1	32.6	18.0	7.7	2.4	154
80°N		41.9	68.5	17.3	14.6			142

Table 11. — Annual ice export across the 81st parallel in 1000 $km^3 s^{-1}$.

Year:	1976	1977	1978	1979	1980	1981	1982	1983	1984
Ice export:	125	154	146	158	158	160	172	173	134

year (Table 10). The ice transport across the 80th parallel is somewhat less, 0.142 mill. $km^3 s^{-1}$. This latitudinal reduction may suggest an effect of melting caused by the warmer West Spitsbergen Current. Observations show that the melting takes place east of the zero meridian (Østlund & Hut 1984). The annual average melting rate then becomes 0.16 cm h^{-1} over the area in question. Preliminary reports on summer melt rates between 0.1 and 1.5 cm h^{-1} in the Fram Strait have been given by Josberger (1984) and Vinje (1984). The above annual average therefore seems to be of a reasonable magnitude.

The latter annual export rate across the 81st paralell, 0.154 mill. $m^3 s^{-1}$, is in close agreement with the former, more directly estimated figure, 0.159 mill. $m^3 s^{-1}$, and lends support to the latter method of estimating the outflow, i.e. with the aid of the atmospheric pressure distribution in the Norwegian-Greenland Sea.

In support of the range of variation, it is noted that the highest monthly maximum, 0.283 mill. $m^3 s^{-1}$ obtained for January (Fig. 23), is similar to the high value of 0.29 mill. $m^3 s^{-1}$, which Wadhams (1983) calculated from a combination of submarine measurements of the ice thickness and previous satellite observations by Vinje (1977) of the drift profile during conditions with relatively high drift speeds.

The maximum range for the interannual ice export through the Fram Strait is 0.048 mill. $m^3 s^{-1}$ (Table 11). The calculations suggest an average increase in the ice export for the period 1976 to 1983 from about 0.13 to 0.17 mill. $m^3 s^{-1}$. The marked decrease of the export in 1984 corresponds to a decrease in the intensity of the atmospheric circulation in the Norwegian-Greenland Sea with which these figures are highly correlated (through Equation (6)).

There are several sources of measurement errors. Taking the seasonal ice thickness variation to be 0.3 m (Nazincev 1971) and adding 0.2 m of equivalent ice for the snow cover (Ivanov 1976; USSR Atlas of the Arctic Ocean 1980; Hanson 1985), the annual range of variation would have increased with about 0.02 mill. $m^3 s^{-1}$. As the standard error of estimate of Umax on ΔP (Equation (6)) is 0.039 m s^{-1} and the volume transport is proportional with Umax, this suggests a standard error of estimate of the ice volume transport on ΔP corresponding to about 0.044 mill. $m^3 s^{-1}$.

The majority of the ice that leaves the Arctic Ocean passes through the Fram Strait. The other passages are too narrow, and more importantly, they are not influenced by an ice-coveying persistent major current. Typically, the ice export through the Canadian Archipelago amounts to only 0.007 mill. $m^3 s^{-1}$ (Sadler 1976), or below 5% of the export through the Fram Strait. The small net import from the Barents Sea amounts to less than 1% of the latter (Vinje 1985).

Our estimate of an annual average ice export rate through the Fram Strait, 0.159 mill. $m^3 s^{-1}$, can be compared with Koerners (1973) value of a total ice export of 0.177 mill. $m^3 s^{-1}$, based on budget calculations from surface observations across the Arctic Ocean, and with 0.165 mill. $m^3 s^{-1}$ of ice equivalent, as calculated by Östlund & Hut (1984) on the basis of the Arctic Ocean mass balance from isotope data. Assuming stationary conditions, our figure is also in fair accordance with the net fresh water input of 0.134 mill. $m^3 s^{-1}$ in ice equivalent due to runoff, precipitation

and evaporation over the Arctic Basin as calculated by Ivanov (1976). To obtain the total fresh water input the effect of the less saline influx of water through the Bering Strait (e.g. Aagaard & Greisman 1975) should for instance also be included. However, because of the uncertainties of the various estimates we shall refrain from a further refinement of the comparison. Moreover, the various calculations suggest an interannual variation of the various fluxes of a magnitude which makes a comparison between averages obtained for different periods questionable.

4. Acknowledgements

The Norwegian Ice Drift Experiment (ICEX) has been funded by the Norwegian National Committee for the Global Atmospheric Research Programme (GARP), the Norwegian Polar Research Institute, and the Norwegian Meteorological Institute. The ICEX capsule was developed in cooperation with, and manufactured by the Chr. Michelsens Institutt. Svalbardfly A/S performed the first buoy deployments on the ice in the central part of the Fram Strait and east of Svalbard in 1976. Since 1978 the buoys have been parachute-dropped by the Norwegian Air Force in the Transpolar Ice Drift Stream at more northern locations. This cooperation made the experiment possible and is greatly appreciated.

The National Aeronautics and Space Administration gave free access and data transfer from their Nimbus-6 location system from 1975 until the positioning system failed in 1980. Since 1981 access to the Service Argos Location System has been funded by the National Oceanic and Atmospheric Administration (NOAA) for which we are very grateful.

The ice drilling teams had a particularly labourious job and we are especially thankful for their endurance. Last but not least we highly appreciate the cooperation with the Alfred-Wegener Institute for Polar Research and we are very thankful to the captains and the crews aboard LANCE and POLARSTERN for their interest and help during the crossings of the East Greenland Ice Drift Stream.

5. References

Aagaard, K. & Coachman, L.K. 1968: The East Greenland Current north of Denmark Strait: Part I and Part II. *Arctic 21 (3 and 4).*

Aagaard, K. 1970: Wind-driven transports in the Greenland and Norwegian Seas. *Deep-Sea Res. 17.*

Aagaard, K. & Greisman P. 1975: Toward New Mass and Heat Budgets for the Arctic Ocean. *J. Geophys. Res. 80(27).*

Ackley, S., Hibler III, W. D., Kugzruk, F., Kovacs, A. & Weeks, W. 1974: Thickness and roughness variations of Arctic multi-year sea ice. *AIDJEX Bulletin 25.* University of Washington.

Bushuev, A.V. 1966: Use of Structure Functions to Determine the Spatial Variability of Ice Thickness. *Trudy 277, Arctic and Antarctic Research Institute (AANI),* Leningrad.

Cavalieri, D. J., Gloersen, P. & Campbell, W. J. 1984: Determination of Sea Ice Parameters with the NIMBUS 7 SMMR. *J. Geophys. Res. 89 (D4).*

Colony, R. & Munoz, E.A. 1985: *Arctic Ocean Buoy Program. Data Report. 1 January 1983 — 31 December 1983.* Polar Science Center. University of Washington.

Colony, R. & Thorndike, A.S. 1983: An estimate of the mean field of Arctic sea ice motion. *J. Geophys. Res. 89(C6).*

Doronin, Yu.P. & Kheisin, D.E. 1975: *Morskoi Led (Sea Ice).* Gidrometeoizdat, Leningrad. (Transl. and publ. for the Office of Polar Program of NSF).

Einarsson, T. 1972: Sea Currents, Ice Drift, and Ice Composition in the East Greenland Current. *In: Sea Ice Proceedings of an International Conference, Reykjavik, Iceland, May 10—13, 1971.*

Felzenbaum, A.I. 1958: The theory of the steady drift of ice and the calculations of the long period mean drift in the central part of the Arctic Basin. Translated from *Problems of the North No. 2,* Leningrad.

Griffiths, R.W. & Linden, P.F. 1982: Laboratory experiments on fronts. Density-driven boundary currents. *Geophys. Astrophys. Fluid Dyn. 19.*

Gordienko, P.A. & Karelin, D.B. 1945: Problemy peremescenija i respredelenja l'dov v Arkticeskom bassejne. *Probl. Arktiki. 3.* Leningrad.

Gordienko, P.A. 1958: Arctic Ice Drift. *Proc.Conf. on Arctic Sea Ice Natl. Acad.Sci., Washington, DC, Publ. No. 598.*

Hanson, A.M. 1985: Observations of Ice and Snow in the Eastern Part of the Chukchi Sea: A Serendiptious Cruise on the POLAR SEA. *MIZEX Bulletin. VI: MIZEX West. CRREL May 1985* (Ed.: P. Wadhams).

Hibler III, W.D. 1979: A dynamic thermodynamic sea ice model for climate studies. *J. Phys. Oceanogr. 9(4).*

Hibler III, W.D. 1980: Modelling a variable thickness sea ice cover. *Monthly Weather review 108(12).*

Hibler III, W.D., Ackley, S.F., Weeks, W.F. & Kovacs, A. 1972: Top and Bottom Roughness of a Multi-year Ice Floe. *AIDJEX Bull. 13,* Div. of Marine Res., Univ. of Wash.

Hibler III, W.D., Mock, S.J. & Tucker III, W.B. 1974: Classification and variation of Sea Ice Ridging in the Western Arctic Basin. *J. Geophys. Res. 79(18).*

Hibler III, W.D. & Bryan, K. 1984: A Large-Scale Ice/Ocean Model for the Marginal Ice Zone. MIZEX Bulletin III: Modeling the Marginal Sea Ice Zone (Ed.: W.D. Hibler III). *CRREL Special Report 84—7.*

Ivanov, V.V. 1976: Fresh water balance of the Arctic Ocean. *Arctic and Antarctic Research Institute, Leningrad, Trudy, 323.*

Johannessen, O.M., Johannessen, J.A., Morison, J., Farrelly, B.A. & Svendsen, E.A.S. 1983: Oceanographic Conditions in the Marginal Ice Zone North of Svalbard in early Fall 1979. With an Emphasis on Mesoscale Processes. *J. Geophys. Res. 88(C5).*

Johnson, W. & Kudo, H. 1962: *The Mechanics of Metal Extrusion.* Manchester University Press, Manchester.

Josberger, E.G. 1984: Preliminary data report. MIZEX 1983 ablation studies. (Not published).

Kiilerich, A. 1945: On the hydrography of the Greenland Sea. *Med. om Grønland 144(2),* København.

Kloster, K. & Rafto, J. 1980: ICEX-Project. Data from drifting buoys north and west of Svalbard in fall of 1979. *Data report No. 851129-1 from Chr. Michelsens Institutt,* Bergen.

Kloster, K. & Svendsen, E. 1982: A NIMBUS-7 SMMR algarithm for sea ice mapping and its application to the NORSEX marginal ice zone experiment. *Report No. 821153-1 from Chr. Michelsens Institutt,* Bergen.

Koerner, R.M. 1973: The mass balance of the sea ice in the Arctic Ocean. *J. Glaciol. 12.*

Laktionov, V.A. & Yanes, A.V. 1960: Okeanograficheskii ocherk severnoi chasti Greenlandskogo moroya. Sovietskie Ribokh. Issled. vMoyakh Evropeiskogo Severa, Moskva, Vniro-Pinro.

Leppäranta, M. 1981: On the structure and mechanics of pack ice in the Bothnian Bay. *Finnish Mar. Res. No. 248.*

Massom, R. 1984: Tabular icebergs off Nordostrundingen, N.E. Greenland. *Iceberg Research. No. 8, Scott Polar Res. Inst.,* October 1984.

Maykut, G.A. & Untersteiner, N. 1971: Some results from a time dependent thermodynamic model of sea ice. *J. Geophys. Res. 76.*

McPhee, M.G. 1980: An analysis of pack ice drift in summer. In Pritchard, R.S. (ed.): *Sea Ice Processes and Models.* University of Washington Press, Seattle.

Nansen, F. 1902: The oceanography of the North Polar Basin. The Norwegian North Polar Expedition 1893—1896. *Sci. Res. 3.*

Nazincev, Ju.L. 1971: Isostatic phenomena on drifting ice floes. *Arctic and Antarctic Research Institute, Trudy 300.* (Transl. at Norsk Polarinstitutt).

Neralla, V.R., Liu, W.S., Venkatesh, S. & Danard, M.B. 1980: Techniques for Predicting Sea Ice Motion. In Pritchard, R.S. (ed.): *Sea Ice Processes and Models.* University of Washington Press.

Nergaard, N., Vinje, T.E. & Finnekåsa, Ø. 1985: Report on ice buoys in the Arctic and the Antarctic. *Report No. 851129-1 from Chr. Michelsens Institutt,* Bergen.

Newton, J.L. 1983: Hydrographic Structure over the Northeast Greenland Shelf. Report on the meeting: The Physical and Chemical Oceanography of the Arctic Ocean. *Special Report No. 1. Oseanografiska Institutionen.* Göteborgs Univ.

Ostenso, A. & Pew, J.A. 1968: Sub-bottom seismic profile of the east coast of Greenland. In: *Arctic Drifting Stations* (Coordinator Sater, J.E.). Arctic Inst. of N. Am., Wash. D.C.

Palfrey Jr., K.M. 1967: *Physical oceanography of the northern part of the Greenland Sea in the summer of 1964.* M.S. Thesis, Univ. of Wash., Seattle.

Palosuo, E. & Leppäranta, M. 1982: Ice conditions between Svalbard and Frans Josef Land on YMER-80 Expedition, July 1980. Symposium Arktis som livsmiljø, Oslo 27—28 Oct., 1982. Not published.

Papanin, J. 1948?: *Life on an Icefloe.* Hutchinson & Co., London (No year of edition, French edition 1948).

Pritchard, R.S., Reimer, R.W. & Coon, M.D. 1979: *Ice flow through Straits. Port and Ocean Engineering under Arctic Conditions 1979.* Norwegian Institute of Techonology, Trondheim.

Reed, R.J. & Campbell, W.J. 1962: The Equilibrium drift of ice station Alpha. *J. Geophys. Res. 67(1).*

Riis-Carstensen, E. 1938: Fremsættelse af et dynamisk-topografisk kort over Østgrønlandsstrømmen mellom 74° og 79° N br. på grundlag af hidtidig gjorte undersøgelser i disse egne. *Geografisk Tidsskrift 41(1).*

Rothrock, D.A. 1986: Ice distribution-measurements and theory. In Untersteiner, N. (ed): *Air-Sea-Ice Interaction. NATO Advanced Study Institute.* In press.

Sadler, H.E. 1976: Water, heat and salt transports through Nares Strait, Ellesmere Land. *J. Fish. Res. Bd. Canada 33(10)*

Shapiro, L.H. & Burns, J.J. 1975: Satellite Observations of Sea Ice Movement in the Bering Strait Region. In Weller, G. & Bowling A.S. (eds.): *Climate of the Arctic.* Geophysical Institute, University of Alaska, Fairbanks.

Shuleikin, V.V. 1938: The drift of ice fields. *Dokl. Akad. Nauk. USSR. 19.*

Smith IV, D.C., Morison, J.H., Johannessen, J.A. & Untersteiner, N. 1984: Topographic Generation of an Eddy at the Edge of the East Greenland Current. *J. Geophys. Res. 89(C 5).*

Strübing, K. 1968: Über Zusammenhänge zwischen der Eisführung des Ostgrönlandstrohms und der atmosphärishen Zirkulation über dem Nordpolarmeer. *Deut. Hydr. Zeit. 20(6).*

Svendsen, E., Kloster, K., Farrelly, B., Johannessen, O. M., Johannessen, J. A., Campbell, W. J., Gloersen, P., Cavalieri, D. & Mätzler, C. 1983: Norwegian Remote Sensing Experiment: Evaluation of the NIMBUS-7 Scanning Multichannel Microwave

Radiometer for Sea Ice Research. *J. Geoph. Res. 88 (C5).*

Symonds, G. & Peterson, I.K. 1985: MIZEX: Ice Floe Trajectories through the Greenland Sea. *Canadian Data Report of Hydrography and Ocean Sciences No. 33.* Dept. of Fisheries and Oceans.

Thorndike, A.S. & Colony, R. 1980: *Arctic Ocean Buoy Program. Data Report 1 January 1979 — 31 December 1979.* Polar Science Center, University of Washington, Seattle.

Thorndike, A.S. & Colony, R. 1981: *Arctic Ocean Buoy Program. Data Report 1 januar 1980—31 December 1980.* Polar Science Center, University of Washington, Seattle.

Thorndike, A.S. & Colony, R. 1982: Sea Ice Motion in Response to Geostrophic Winds. *J. Geophys. Res. 87(C8).*

Thorndike, A.S., Colony, R. & Muños, E.A. 1982: *Arctic Ocean Buoy Program. Data Report 1 Januar 1981—31 December 1981.* Polar Science Center, University of Washington, Seattle.

Thorndike, A.S., Colony R. & Muños, E. 1983: *Arctic Ocean Buoy Program. Data Report 1 January—31 December 1982.* Polar Science Center, University of Washington.

USSR Ministry of Defence 1980: *Atlas of Oceans. The Arctic Ocean.* (Eds.: S.G. Gorskov and V.I. Faleev).

Vinje. T. 1970: Some observations of the ice drift in the East Greenland Current. *Norsk Polarinstitutt Årbok 1969.*

Vinje, T. 1976: Sea ice conditions in the European sector of the marginal seas of the Arctic, 1966—1975. *Norsk Polarinstitutt Årbok 1975.*

Vinje, T.E. 1977: Sea ice studies in the Spitsbergen-Greenland area. *Landsat Report E77-10206.* US Dep. of Com. Natl. Tech. Info. Service, 5285 Port Royal Road, Springfield, VA.

Vinje, T.E. 1980: On the extreme sea ice conditions observed in the Greenland and Barents Seas in 1979. *Norsk Polarinstitutt Årbok 1979.*

Vinje, T.E. 1982: The drift pattern of sea ice in the Arctic with particular reference to the Atlantic approach. In Rey, L. & Stonehouse, B. (Eds.): *The Arctic Ocean.* Macmillan, London.

Vinje, T.E. 1984: The Fram Strait Cruise with M/S LANCE 17—31 August 1984. *Norsk Polarinstitutt Rapportserie Nr. 18.*

Vinje, T.E. 1985: Drift, composition, morphology and distribution of the sea ice fields in the Barents Sea - long term observations. *Norsk Polarinstitutt Skrifter No. 179C.*

Vinje, T.E. & Steinbakke, P. 1976: Nimbus-6 located automatic stations in the Svalbard waters in 1975. *Norsk Polarinstitutt Årbok 1975.*

Vinje, T. & Finnekåsa, Ø. 1986: Norwegian ice drift experiment. Buoy drift data 1976—1979. *Norsk Polarinstitutt Rapport No. 28.*

Vize, V. Ju. 1937: Ice drift from the Kara Sea into the Greenland Sea. *Problems of the Arctic. No 1.* Leningrad.

Volkov, N.A. & Gudkovic, I.M. 1967: Osnovnye itogi izucenija dreifa l'dov v Articeskom bassejne. *Probl. Arkt. i Antark. 27.* (Transl. at Norsk Polarinstitutt).

Vowinckel, E. 1964: Ice transport in the East Greenland Current and its causes. *Arctic 17(2).*

Wadhams, P. 1981a: Sea Ice Topography of the Arctic Ocean in the Region 70° W to 25° E. *Phil. Trans. Roy. Soc. London 302(1464).*

Wadhams, P. 1981b: The Ice Cover in the Greenland and Norwegian Seas. *Reviews of Geophysics and Space Physics 19(3).*

Wadhams, P. 1983: Sea ice thickness distribution in Fram Strait. *Nature 305(5930).*

Wadhams, P., Gill, A.E. & Linden, P.F. 1979: Transects by submarine of the East Greenland Polar Front. *Deep Sea Res. 26(12 A).*

Wadhams, P. & Squire, V.A. 1983: An Ice-Water Vortex at the Edge of the East Greenland Current. *J. Geophys. Res. 88(C 5).*

Wittman, W.I. & Schule, J.J. 1966: Comments on the Mass Budget of Arctic Pack Ice. *Proc. of the Symp. on the Arctic Heat Budget and Atmos. Circulation.* The Rand Corporation, Santa Monica.

Yakovlev, G.N. 1955: Nivelirovochnyye raboty pa izucheniya morfologii ledyanqgo pokvova. (Study of the morphology of the icecover by surveying). «Morskoi Transport», Leningrad. *(Transl. Amer. Met Soc. ASTIA Doc. AD 117136).*

Zacharov, V.F. 1976: Pocholodanie Arktiki i ledjanoj pokrov arktischeskich morej (Cooling of the Arctic and the ice cover of the Arctic Seas). *AANI Trudy 337.* Gidrometeoizdat, Leningrad. (Transl. at Norsk Polarinstitutt).

Zubov, N.N. 1943: L'dy Arktiki. Glavsevmorput, Moskva. *(Transl. U.S. Navy Electr. Lab: Arctic Ice, Sea Ice.)*

Zubov, N.N. & Somov, M.M. 1940: The ice drift of the central part of the Arctic Basin. *Probl. Arkt. 2* (Am. Met. Soc. TR27).

Östlund, G.H. & Hut, G. 1984: Arctic Ocean Water Mass Balance From Isotope Data. *J. Geophy. Res. Vol. 89(C4).*

ISBN 82-90307-44-6
Printed July 1986